Seismological investigations in the Gioia Tauro Basin (southern Calabria, Italy)

Elisabetta Giampiccolo ([1]), **Carla Musumeci** ([1]), **Filippo Falà** ([2]) **and Stefano Gresta** ([2])
([1]) Istituto Nazionale di Geofisica e Vulcanologia, Sezione di Catania, Catania, Italy
([2]) Dipartimento di Scienze Geologiche, Università degli Studi di Catania, Italy

Abstract
This study provides new seismological information to characterize the seismically active area of the Gioia Tauro basin (southern Calabria, Italy). Seismic activity recorded by a temporary network from 1985 to 1994 was analyzed for focal mechanisms, stress tensor inversion, P-wave seismic attenuation and earthquake source parameters estimation. Fault plane solutions of selected events showed a variety of different mechanisms, even if a prevalence of normal dip-slip solutions with prevalent rupture orientations occurring along ca. NE-SW directions was observed. Stress tensor inversion analysis disclosed a region governed mainly by a NW-SE extensional stress regime with a nearly vertical σ_1. These results are consistent with the structure movements affecting the studied area and with geodetic data.
Furthermore, evaluation of P-waves seismic attenuation and earthquake source parameters of a subset of events highlighted a strong heterogeneity of the crust and the presence of fault segments and/or weakened zones where great stress accumulation or long-rupture propagation are hindered.

Key words *Southern Calabria – Seismicity – Stress tensor – Attenuation – Source parameters*

1. Introduction

The Calabrian arc (fig. 1) is the most arcuate southern part of the Mediterranean orogenic belt. The arc connects the E-W and the NW-SE trending branches of the belt, which are represented by the Maghrebian and the southern Apennines chains, respectively. The most impressive tectonic feature of the arc is a prominent normal fault belt that extends, more or less continuously, for a total length of about 180 km along the inner side of the arc (Tortorici *et al*., 1995). The morphological features of the fault escarpments suggest slip rates of 0.8-1.1 mm/yr for the last 700 k.y. and values of 0.6-0.9 mm/yr for the last 120 k.y., indicating a uniform rate of faulting since the Middle Pleistocene (Tortorici *et al*., 1995). The different normal fault segments separate the main Pliocene-Pleistocene basins from the uplifted mountain ranges (Tortorici *et al*., 1995). The study area (fig. 1) is a ca. 40 km long section of the Calabrian arc that includes the Gioia-Tauro basin and the Aspromonte mountain range. In particular, the Gioia Tauro basin (fig. 1) is part of a system of basins that border the Serre-Aspromonte toward the western coast of southern Italy. It is characterized by the Cittanova fault (hereafter referred as CF), a well exposed west dipping high-angle normal fault about 20 km long, which separates metamorphic and igneous rocks to the east from sedimentary marine and continental successions to the west (Galli and Bosi, 2002). In the field, the CF appears both as a single ~10 m high scarp or as smaller multiple

Mailing address: Dr. Elisabetta Giampiccolo, Istituto Nazionale di Geofisica e Vulcanologia, Sezione di Catania, Piazza Roma 2, 95123 Catania, Italy; e-mail: giampiccolo@ct.ingv.it

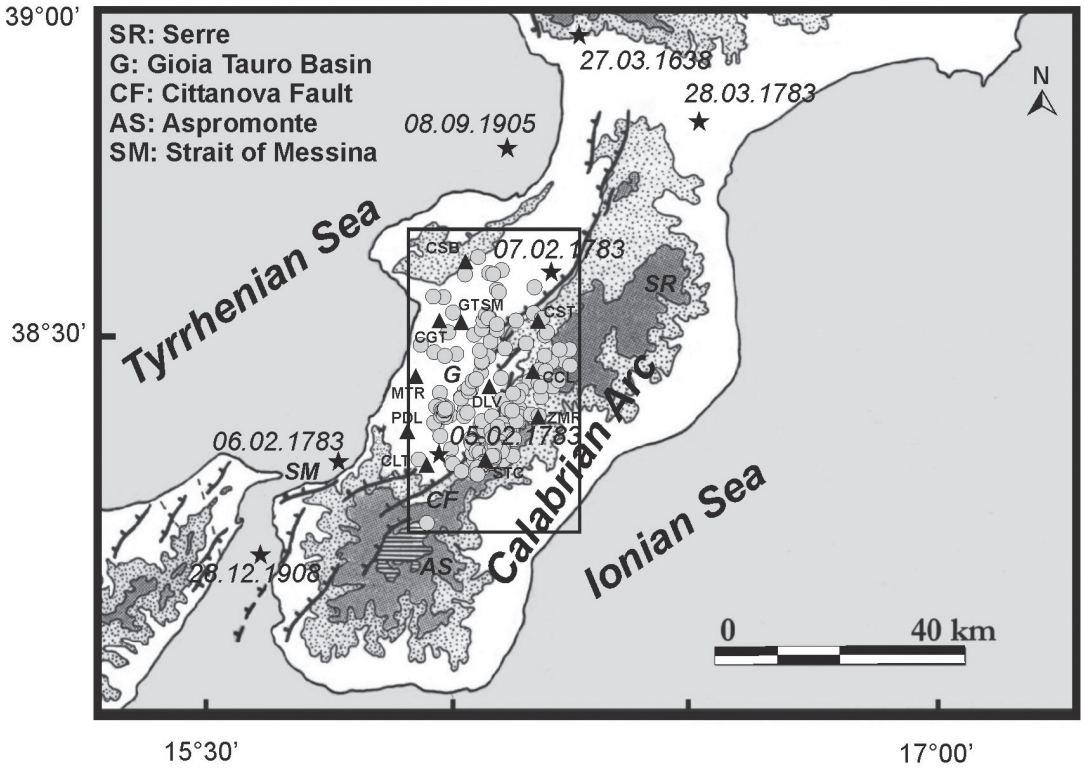

Fig. 1. Map of the study area (modified after Tortorici *et al*., 1995) showing the location of the events selected in this study (grey circles inside the black rectangle). Historical earthquakes are also shown (stars). Triangles represent the stations of the seismic network operating from 1985 to 1994.

scarpets, with a 1 to 3 m high frontal scarp that, in some places, has a free face (Wallace, 1977). It is composed of a dozen *en echelon* strands, 1-3 km long which strike N40°E, with the exception of two N25°E relay ramps. Almost all the strands show a right step with respect to the northern ones (Galli and Bosi, 2002).

From a seismic point of view, the Calabrian arc represents one of the most active zones in Europe. It has experienced the strongest earthquakes affecting the Italian region over the last 3 centuries (fig. 1): 1638 (Io=IX MCS), 1783 (Io=X-XI MCS), 1905 (Io=X-XI MCS), 1908 (Io=XI MCS) (*e.g*. Boschi *et al*., 2000; Monaco and Tortorici, 2000; Galli and Bosi, 2003). The strongest events (except those of 1638) occurred in the southern sector, between the Messina and Catanzaro straits. In particular, the 1783 earthquakes were a catastrophic and destructive sequence for an area more than 100 km in length and 30 km in width (Tyrrhenian coast and front of the Aspromonte-Serre Range). The CF is generally identified as the superficial expression of the seismogenetic structure of the February 5, 1783 earthquake (Galli and Bosi, 2002). However, the lack of geological evidence concerning middle-upper Pleistocene activity of the CF has led some authors to question its present activity and to search for another seismic source elsewhere. Valensise and D'Addezio (1994), among others, claim that the CF is the fossil trace of an inactive fault, or an ancient coast line. The authors assume that the fault controlling the geometry and the seismicity of the Gioia Tauro basin is instead a blind, low-angle, east dipping fault system (Gioia

Tauro Fault). According to recent paleoseismological and archeoseismological studies (*e.g.* Galli and Bosi, 2002) the CF is still active and has produced several significant events in the Holocene and historical times.

The occurrence in the Calabrian arc of both intense Quaternary faulting and active crustal seismicity suggests that these phenomena might be related to each other. Therefore, with the aim of monitoring the seismic activity of the Gioia Tauro basin, a local seismic network was managed, on behalf of ENEL (Italian national electricity board), from April 1985 to April 1994 by ISMES (Istituto Sperimentale Modelli E Strutture), which provided for a catalogue of the recorded seismicity too. Despite the large amount of recorded local earthquakes over a 9-year time span, little effort has been made so far to carry out detailed researches on seismological topics. Recently, Raffaele *et al*. (2006) investigated the three-dimensional velocity structure of the Gioia Tauro basin providing important constraints on the structural and geological features. However, more studies and researches are needed to better understand and explain both tectonics and physical mechanisms occurring in this seismically active area. As is known, the assessment of seismic hazard requires information on both the nature of the earthquake source and on the medium where seismic waves propagate. In this framework, we attempt a systematic and detailed analysis of a 9-year time span, which includes the most complete and largest dataset available to date in southern Calabria. Our goals are: i) to provide a dataset of well-constrained fault plane solutions and source parameters for a selected subset of earthquakes; ii) to give information on the distribution of stress direction and discuss the results in terms of spatial earthquake distribution and tectonics; iii) to obtain a first estimate of the seismic attenuation of P-waves which may provide important insights into the nature of heterogeneities in the study area.

2. Instruments and Data

A seismic network of 11 stations was installed in the Gioia Tauro basin between April 1985 and April 1994. Until July 1992 the network was equipped with one three component (DLV) and ten vertical component stations. After July 1992 also PDL and CST were run as three component seismic stations (Raffaele *et al*., 2006). Each station was equipped with Mark L4C and Mark L4C-3D seismometers (flat response between 0.8 and 30 Hz; Moia, 1987) having a natural frequency of 1 Hz and a damping of 70% of critical. The data were sampled with a sampling rate of 153.8 Hz.

Among 3741 events recorded during the 9 years of the network's operation, we selected a subset of 252 events from the ISMES catalogue within an area defined by a rectangle with coordinates 38.16-38.65 latitude N° and 15.89-16.30 longitude E° (fig. 1). The quality of the input data was improved by repicking the P- and S-phases. The earthquakes were then relocated (table I) using the Hypoellipse code (Lahr, 1989) and the minimum 1D velocity model proposed by Raffaele *et al*. (2006). Final locations are affected by uncertainty less than 2 km in epicentral coordinates (80% Erh≤1.0 km), less than 3 km in focal depths (50% Erz≤1.0 km), and root-mean-square (rms) traveltime residual less than 0.25 s. Higher depth errors are mainly observed for the events occurring along the western coastal sector of the study area because of the largest azimuthal gaps. Since high-precision hypocentral coordinates and reliable error-estimates are crucial for seismo-tectonic interpretation, we used the differences between minimum 1D and 3D model locations (Raffaele *et al*., 2006) to verify the accuracy of hypocentral coordinates. These location differences are rather small with an average location accuracy of about 0.3 km in horizontal directions and about 0.8 km in depth for the selected well locatable events.

The spatial distribution of seismicity shows an Appenninic trend along a NE-SW direction (fig. 1). The hypocentral distribution of the events extends to about 25 km, with depth mainly concentrated from 10 to 25 km. The local magnitude (M_L) of the events was calculated following the procedure implemented in the Hypoellipse code (Lahr, 1989) which proved to give very similar magnitude values to those calculated following the standard Richter

Table I. Location parameters of the 252 events selected from the ISMES catalogue, including local magnitude (M_L), number of data (N), azimuthal gap (Gap), squared residual travel times (rms), Erh and Erz.

N°	Date	Orig. Time	M_L	Lat. N°	Long. E°	Depth	N	Gap	rms	Erh	Erz
1	14/04/1985	03:31:22.04	0.5	38.310	16.038	18.75	8	119	0.06	0.8	1
2	28/04/1985	22:01:49.64	0.5	38.376	15.994	13.5	7	127	0.08	0.7	0.7
3	28/04/1985	22:19:51.32	0.7	38.378	15.995	13.75	7	99	0.06	0.7	0.7
4	28/04/1985	22:41:03.14	1.4	38.374	15.991	13.43	10	128	0.07	0.5	0.7
5	20/05/1985	01:45:07.67	0.5	38.372	15.931	20.27	8	200	0.04	1	0.8
6	27/06/1985	22:27:58.56	2.0	38.405	16.016	58.13	9	89	0.09	1.8	2.1
7	19/07/1985	07:56:06.96	0.5	38.281	15.954	10.28	6	184	0.05	1.7	2.6
8	24/08/1985	17:56:37.65	1.0	38.319	16.019	12.59	8	132	0.07	1	1.9
9	31/08/1985	21:22:08.53	0.5	38.470	15.948	15.09	6	106	0.06	0.7	2.1
10	26/10/1985	16:52:03.04	1.2	38.279	16.008	17.47	8	117	0.05	0.9	1.3
11	27/10/1985	06:44:54.88	1.5	38.277	16.007	17.22	7	120	0.05	1	1.4
12	28/10/1985	18:41:47.79	2.2	38.294	16.047	18.88	11	149	0.07	1	1.3
13	13/11/1985	13:29:46.27	0.5	38.455	16.036	0.74	6	159	0.14	0.7	3
14	20/11/1985	17:07:22.24	1.7	38.288	16.038	18.49	9	143	0.05	0.7	0.8
15	11/12/1985	22:11:23.52	1.2	38.571	16.059	22.77	8	222	0.04	1	1
16	26/12/1985	00:46:51.07	0.6	38.361	16.059	20.63	8	80	0.04	0.8	0.8
17	27/12/1985	09:56:21.52	1.2	38.258	16.025	19.64	6	272	0.02	1.1	1.3
18	27/12/1985	18:00:10.63	2.0	38.263	16.024	19.33	11	214	0.06	0.7	0.8
19	27/12/1985	20:05:48.43	0.6	38.254	16.02	19.16	6	245	0.01	1.1	1.4
20	27/12/1985	20:07:31.85	1.2	38.264	16.02	19.33	9	176	0.05	0.7	0.9
21	27/12/1985	20:07:49.31	1.4	38.261	16.032	18.27	10	219	0.12	0.7	0.8
22	28/12/1985	14:52:24.25	1.9	38.264	16.026	19.79	10	214	0.06	0.7	0.8
23	29/12/1985	19:56:02.99	1.0	38.258	16.022	18.8	7	243	0.01	0.9	1.1
24	04/01/1986	02:37:06.54	1.6	38.262	16.023	19.02	11	215	0.06	0.7	0.8
25	30/01/1986	06:22:10.86	1.5	38.307	16.075	20.12	7	187	0.1	1.2	1.2
26	04/02/1986	22:44:05.52	0.7	38.322	16.06	16.56	6	125	0.04	1.3	2.2
27	05/02/1986	00:00:30.34	0.8	38.311	16.067	19.63	8	148	0.05	0.8	0.8
28	23/02/1986	15:33:29.42	1.5	38.260	16.022	19.21	8	221	0.02	0.8	0.9
29	23/02/1986	15:33:47.76	1.5	38.263	16.031	18.08	9	216	0.1	0.8	1.1
30	23/02/1986	15:42:31.76	1.2	38.260	16.029	18.23	9	218	0.1	0.8	1
31	24/02/1986	10:09:56.51	1.5	38.266	16.017	18.78	10	150	0.1	0.6	0.8
32	08/03/1986	03:11:28.64	1.3	38.263	16.029	18.1	12	216	0.09	0.7	0.7
33	08/03/1986	17:39:09.65	1.0	38.263	16.028	19.1	9	215	0.06	0.7	0.8
34	12/03/1986	03:34:09.64	2.4	38.260	16.022	18.66	11	206	0.08	0.7	0.8
35	12/03/1986	03:34:13.93	2.2	38.261	16.026	18.66	11	206	0.08	0.7	0.8

Table I. (*continued*).

N°	Date	Orig. Time	M_L	Lat. N°	Long. E°	Depth	N	Gap	rms	Erh	Erz
36	12/03/1986	03:36:04.43	2.2	38.262	16.027	18.64	11	204	0.07	0.7	0.8
37	12/03/1986	03:39:14.88	1.1	38.256	16.026	19.29	7	222	0.04	0.9	1.4
38	12/03/1986	03:54:00.19	1.9	38.259	16.022	18.87	11	217	0.06	0.7	0.8
39	12/03/1986	05:00:06.66	1.0	38.250	16.02	17.29	8	248	0.06	0.8	1
40	12/03/1986	05:49:58.83	0.9	38.257	16.022	18.89	6	244	0.02	1	1.5
41	12/03/1986	05:53:25.81	2.1	38.260	16.021	18.66	11	216	0.07	0.7	0.8
42	12/03/1986	06:58:59.54	1.7	38.257	16.017	18.61	9	213	0.07	0.7	0.8
43	12/03/1986	09:27:21.56	1.5	38.265	16.026	19.28	9	170	0.06	0.7	0.8
44	12/03/1986	15:21:38.95	1.4	38.261	16.022	19.11	9	216	0.06	0.7	0.9
45	12/03/1986	18:55:09.54	1.5	38.263	16.023	18.94	10	214	0.06	0.7	0.8
46	21/03/1986	06:01:18.65	1.9	38.261	16.02	19.28	10	215	0.06	0.7	0.8
47	01/04/1986	22:04:28.45	1.1	38.465	16.149	24.52	9	201	0.03	0.8	0.9
48	13/04/1986	03:56:22.62	1.0	38.431	16.031	17.18	6	162	0.01	1.5	1
49	17/06/1986	18:46:00.44	2.0	38.566	16.033	21.49	10	199	0.04	0.7	1
50	17/07/1986	07:30:31.86	1.2	38.257	16.023	18.72	7	244	0.02	0.9	1.1
51	29/07/1986	19:19:28.52	1.0	38.319	15.924	21.2	9	77	0.06	0.7	0.9
52	02/08/1986	11:20:52.40	0.9	38.324	15.92	22.01	6	127	0.04	1.1	1.1
53	02/08/1986	12:27:39.72	0.9	38.324	15.919	21.85	6	164	0.03	1.5	1.2
54	08/08/1986	19:30:52.80	0.6	38.284	16.04	19.47	6	155	0.02	0.9	1.1
55	24/08/1986	02:38:37.50	1.1	38.286	16.018	12.81	9	104	0.07	0.6	0.9
56	24/08/1986	02:52:31.69	1.1	38.257	16.023	18.27	8	244	0.02	0.8	0.9
57	24/08/1986	20:13:25.54	1.5	38.273	16.022	16.78	8	110	0.06	0.7	1.1
58	26/08/1986	06:54:18.47	1.6	38.263	16.028	19.54	8	215	0.07	0.8	1.1
59	26/08/1986	14:15:29.71	1.1	38.265	16.027	18.9	8	177	0.07	0.8	1.1
60	23/09/1986	20:20:35.27	1.1	38.365	16.141	15.37	8	191	0.06	0.7	0.8
61	19/10/1986	04:09:52.22	1.3	38.264	16.017	21.88	7	172	0.08	0.9	1.1
62	19/10/1986	23:38:14.83	1.0	38.264	15.887	15.27	6	214	0.05	1.5	1.8
63	20/10/1986	13:17:04.23	1.2	38.380	15.99	12.83	8	123	0.12	0.8	0.7
64	27/11/1986	19:26:51.38	1.1	38.251	16.009	21.16	8	223	0.06	0.9	1.2
65	13/12/1986	00:25:35.03	1.2	38.336	15.952	20.72	10	114	0.08	0.7	0.8
66	14/12/1986	01:08:56.81	0.7	38.391	16.117	9.58	6	148	0.02	0.9	1.9
67	16/12/1986	02:13:16.01	1.7	38.335	16.136	19.73	10	206	0.07	0.7	0.8
68	19/03/1987	20:23:05.35	0.7	38.424	16.189	9.96	7	238	0.09	0.8	1.3
69	14/04/1987	13:49:22.08	0.5	38.343	15.982	14.28	6	148	0.1	1.4	3
70	14/04/1987	13:53:47.53	1.4	38.334	15.981	21.28	9	101	0.04	0.9	1.1
71	16/04/1987	09:12:42.77	1.1	38.340	15.988	19.31	6	146	0.02	1.2	1.6

Table I. (*continued*).

N°	Date	Orig. Time	M_L	Lat. N°	Long. E°	Depth	N	Gap	rms	Erh	Erz
72	03/05/1987	04:07:40.12	1.7	38.592	16.01	20.94	9	235	0.08	0.8	1.1
73	12/05/1987	11:34:11.23	1.2	38.423	16.152	18.96	6	285	0	1.3	0.9
74	12/05/1987	11:36:06.70	1.4	38.420	16.145	18.97	7	281	0.04	1.3	0.8
75	12/05/1987	12:11:15.13	1.1	38.409	16.142	18.46	8	220	0.05	0.8	0.8
76	12/05/1987	12:11:59.94	1.4	38.407	16.147	19.3	6	194	0.04	1.2	1.3
77	12/05/1987	12:14:59.85	1.7	38.410	16.144	18.28	10	191	0.07	0.7	0.7
78	12/05/1987	12:17:39.33	1.5	38.404	16.141	17.67	11	188	0.09	0.7	0.7
79	12/05/1987	12:27:26.53	1.2	38.427	16.15	18.46	6	285	0.02	1.6	0.9
80	12/05/1987	12:28:38.11	2.0	38.409	16.137	17.7	11	183	0.06	0.7	0.7
81	12/05/1987	14:58:19.51	1.1	38.422	16.163	17.07	9	213	0.12	0.8	0.8
82	16/05/1987	01:14:47.55	1.3	38.489	16.089	21.78	8	132	0.05	0.8	0.9
83	16/05/1987	10:59:31.36	1.3	38.407	16.15	18.52	9	198	0.05	0.7	0.9
84	14/06/1987	18:24:08.19	2.0	38.442	16.2	21.06	10	236	0.08	1	0.8
85	28/07/1987	20:04:14.44	1.4	38.527	15.938	21.16	9	191	0.1	0.7	1.1
86	28/07/1987	20:05:59.39	0.9	38.528	15.917	19.4	6	209	0.04	1	1.7
87	19/08/1987	23:21:19.28	0.5	38.300	16.07	19.45	6	203	0.02	1	0.9
88	20/10/1987	20:06:39.73	1.2	38.474	16.049	20.8	7	159	0.01	1	1.1
89	18/12/1987	21:17:29.50	1.3	38.259	15.955	22.24	7	180	0.04	1.5	1.2
90	24/01/1988	01:50:50.12	3.0	38.350	15.941	18.55	8	79	0.05	0.7	2.5
91	24/01/1988	18:45:36.87	1.7	38.348	15.936	20.67	8	83	0.06	0.8	0.8
92	25/01/1988	16:24:37.82	1.7	38.352	15.93	21.29	7	89	0.03	0.9	0.9
93	27/01/1988	07:35:41.80	1.6	38.350	15.923	19.68	6	96	0.05	1	1.2
94	27/02/1988	05:11:14.75	1.5	38.333	15.943	21.36	6	188	0.04	1.4	0.9
95	17/04/1988	11:32:41.56	2.9	38.374	15.982	60.65	9	84	0.08	1.9	1.1
96	02/05/1988	02:41:02.81	1.6	38.346	16.072	16.95	8	170	0.04	0.7	0.7
97	15/06/1988	00:22:02.52	1.3	38.376	16.1	19.38	6	176	0.03	1.1	0.8
98	17/07/1988	02:32:13.27	0.9	38.298	15.995	20.57	7	102	0.04	0.9	1.1
99	17/07/1988	17:52:28.66	0.8	38.298	15.995	20.37	6	125	0.04	1.1	1.8
100	19/07/1988	09:50:24.37	1.3	38.347	16.095	15.62	6	193	0.07	0.9	0.9
101	21/07/1988	10:18:59.62	1.3	38.396	16.058	16.23	7	166	0.05	0.9	0.7
102	25/09/1988	02:37:02.95	0.6	38.292	15.996	21.6	7	103	0.05	1	1.8
103	18/11/1988	09:44:31.51	1.3	38.344	15.935	21.08	10	84	0.05	0.6	0.8
104	22/12/1988	11:13:50.37	1.2	38.543	16.127	23.98	6	244	0.02	1.1	1.3
105	11/01/1989	11:36:36.58	1.1	38.263	16.063	18.97	6	232	0.03	0.9	1.2
106	29/01/1989	19:50:47.89	0.7	38.466	16.002	14.74	11	85	0.06	0.6	1.3
107	07/03/1989	18:52:03.75	1.0	38.293	16.055	18.66	6	161	0.05	1.1	1.3

Table I. (*continued*).

N°	Date	Orig. Time	M_L	Lat. N°	Long. E°	Depth	N	Gap	rms	Erh	Erz
108	09/03/1989	16:41:41.39	1.5	38.442	16.179	19.29	7	235	0.06	0.9	0.8
109	29/05/1989	18:59:47.09	1.0	38.332	16.088	18.35	7	128	0.05	0.9	1.4
110	30/05/1989	00:33:46.14	0.7	38.329	16.093	19.54	6	136	0.04	1	1.2
111	04/06/1989	02:20:47.67	1.1	38.332	16.092	19.15	8	130	0.05	0.8	0.8
112	04/06/1989	22:36:21.41	1.5	38.332	16.091	19.11	9	130	0.06	0.7	0.7
113	04/06/1989	22:58:02.94	1.0	38.331	16.093	19.45	9	132	0.06	0.7	0.7
114	04/06/1989	23:56:18.07	1.2	38.331	16.094	19.51	9	132	0.05	0.7	0.7
115	04/06/1989	23:57:03.76	1.6	38.333	16.094	19.65	10	130	0.06	0.7	0.7
116	05/06/1989	04:09:21.01	1.6	38.332	16.093	19.78	10	131	0.06	0.7	0.7
117	06/06/1989	00:06:36.62	1.1	38.338	16.097	19.94	7	118	0.08	0.9	0.9
118	14/06/1989	20:20:22.97	0.6	38.332	16.095	19.08	11	131	0.07	0.7	0.6
119	14/06/1989	21:01:00.28	0.8	38.330	16.095	19.53	9	136	0.06	0.7	0.7
120	14/06/1989	21:18:58.92	1.5	38.326	16.092	19.37	8	141	0.04	0.7	0.8
121	14/06/1989	22:42:35.30	0.7	38.331	16.095	19.05	9	133	0.07	0.7	0.7
122	17/06/1989	04:11:00.73	1.6	38.326	16.094	19.43	7	144	0.04	0.8	0.8
123	17/06/1989	12:37:13.22	0.9	38.334	16.095	19.82	7	126	0.05	1.1	1
124	24/06/1989	01:03:57.11	0.5	38.326	16.09	19.49	7	140	0.04	0.8	0.8
125	21/08/1989	13:52:17.92	1.3	38.421	16.018	15.42	6	155	0.02	1	1
126	21/08/1989	13:58:04.08	1.1	38.423	16.018	15.78	7	157	0.03	0.9	0.7
127	26/08/1989	09:40:08.65	1.4	38.161	15.904	16.61	6	305	0.05	1.2	1.8
128	13/12/1989	18:35:49.30	1.9	38.366	16.093	11.14	10	104	0.04	0.5	0.6
129	21/12/1989	09:00:32.11	1.5	38.270	16.082	18.8	8	228	0.06	0.8	0.8
130	21/12/1989	11:20:23.95	2.2	38.264	16.002	16.58	9	173	0.05	0.7	0.8
131	21/12/1989	12:21:35.23	1.6	38.243	16.003	21.54	7	230	0.06	0.9	1.2
132	22/12/1989	11:20:46.12	1.2	38.240	16.009	21.21	7	234	0.05	1	1.4
133	31/01/1990	21:38:04.83	1.2	38.494	16.03	21.58	7	116	0.02	1	1.3
134	31/01/1990	21:38:17.50	1.8	38.491	16.024	21.71	10	111	0.03	0.6	0.9
135	01/02/1990	00:40:40.35	2.1	38.489	16.025	21.85	11	109	0.04	0.6	0.8
136	01/02/1990	00:47:27.58	1.6	38.491	16.029	21.94	11	113	0.03	0.7	0.7
137	01/02/1990	01:31:18.08	1.5	38.489	16.026	21.61	9	110	0.03	0.7	1
138	01/02/1990	03:17:57.13	2.1	38.489	16.025	21.73	10	110	0.03	0.6	0.9
139	01/02/1990	03:25:16.57	1.3	38.490	16.026	21.41	9	111	0.02	0.7	1
140	01/02/1990	03:36:09.93	1.2	38.490	16.025	22.01	10	110	0.03	0.6	0.9
141	01/02/1990	04:43:30.58	1.9	38.489	16.024	21.93	10	109	0.03	0.6	0.9
142	01/02/1990	04:53:20.05	1.3	38.490	16.028	21.01	8	112	0.02	1.1	1.3
143	01/02/1990	05:04:25.49	1.1	38.491	16.029	21.66	8	113	0.02	1.1	1.3

Table I. (*continued*).

N°	Date	Orig. Time	M_L	Lat. N°	Long. E°	Depth	N	Gap	rms	Erh	Erz
144	01/02/1990	05:46:02.16	2.1	38.489	16.023	22.23	11	109	0.04	0.6	0.9
145	01/02/1990	06:12:50.19	1.6	38.488	16.024	21.92	10	108	0.03	0.6	0.9
146	01/02/1990	06:54:18.82	1.9	38.487	16.023	22.12	10	107	0.03	0.6	0.9
147	01/02/1990	07:46:38.53	1.6	38.489	16.024	22.53	8	109	0.03	0.7	1
148	01/02/1990	08:56:54.99	1.6	38.475	16.018	16.04	10	95	0.07	0.5	1.2
149	01/02/1990	18:44:58.38	2.0	38.489	16.024	21.89	12	109	0.04	0.6	0.8
150	02/02/1990	02:48:35.13	2.0	38.490	16.024	21.35	12	110	0.05	0.6	0.8
151	02/02/1990	05:41:31.89	1.9	38.489	16.024	21.37	11	109	0.03	0.6	0.9
152	02/02/1990	20:12:47.40	1.1	38.494	16.033	21.18	8	118	0.02	0.9	1
153	02/02/1990	23:01:36.98	0.6	38.391	15.999	13.24	10	62	0.05	0.4	0.6
154	02/02/1990	23:01:57.77	0.8	38.394	16.006	13.49	6	154	0.03	0.8	0.7
155	03/02/1990	23:25:23.83	1.1	38.489	16.021	22.16	11	108	0.06	0.6	0.9
156	11/02/1990	21:02:30.34	1.1	38.498	16.026	22.65	6	193	0.02	1.1	1.8
157	11/02/1990	21:29:07.67	1.2	38.493	16.031	21.56	7	115	0.02	0.8	1.1
158	28/02/1990	22:09:46.68	2.4	38.444	16.066	20.96	12	79	0.05	0.6	0.7
159	12/03/1990	19:10:16.12	1.3	38.501	16.125	22.51	9	204	0.03	0.9	0.9
160	16/05/1990	21:33:08.97	1.1	38.245	15.976	21.14	6	216	0.05	1.1	1.3
161	10/06/1990	03:35:05.70	1.8	38.435	15.965	16.08	12	91	0.07	0.4	0.7
162	10/07/1990	20:03:40.77	1.0	38.297	16.085	20.56	7	188	0.06	0.9	1.1
163	29/09/1990	20:39:35.05	2.2	38.382	16.165	16.06	11	218	0.08	0.7	0.6
164	29/09/1990	21:39:11.39	2.5	38.388	16.136	11.97	11	181	0.07	0.5	1
165	29/09/1990	23:47:34.17	1.1	38.392	16.177	12.82	6	228	0.17	1	1.1
166	26/11/1990	03:27:20.77	1.6	38.470	16.153	20	8	205	0.04	1.2	0.8
167	10/12/1990	04:15:15.48	1.4	38.539	16.049	24.76	8	205	0.06	1.1	1
168	31/01/1991	06:57:55.05	2.0	38.371	16.083	13.39	6	93	0.02	1	2.1
169	10/03/1991	10:35:10.98	1.7	38.432	16.148	9.12	10	197	0.12	1.1	1.2
170	20/04/1991	03:26:20.14	1.5	38.345	15.938	21.67	8	129	0.06	0.9	1.1
171	24/09/1991	19:52:59.67	1.6	38.564	16.041	18	6	201	0.06	1.5	2
172	25/09/1991	20:14:56.94	1.7	38.493	16.143	17.86	7	244	0.08	1.6	1
173	29/11/1991	13:54:26.37	1.6	38.257	15.958	10.35	6	186	0.07	1.9	2
174	13/12/1991	21:51:57.84	1.5	38.564	15.983	15.82	7	149	0.07	1.4	1.4
175	19/04/1992	02:35:55.35	2.2	38.283	16.061	19.86	12	187	0.07	0.7	0.7
176	20/04/1992	05:19:12.00	2.0	38.277	16.059	19.97	10	197	0.07	0.7	0.8
177	16/05/1992	02:22:27.20	1.9	38.334	16.039	57.34	9	99	0.04	1.7	1.1
178	16/05/1992	02:52:56.20	1.4	38.483	16.049	21.73	10	112	0.02	0.6	0.8
179	23/05/1992	01:04:56.21	2.3	38.470	15.948	13.59	12	105	0.12	0.6	0.9

Table I. (*continued*).

N°	Date	Orig. Time	M_L	Lat. N°	Long. E°	Depth	N	Gap	rms	Erh	Erz
180	08/07/1992	05:35:54.28	2.1	38.287	16.045	16.95	11	187	0.14	1.5	0.8
181	02/08/1992	00:03:15.14	1.2	38.274	15.999	14.92	6	139	0.14	1.2	2.1
182	03/08/1992	04:37:14.52	1.9	38.280	16.013	13.24	11	103	0.14	0.7	0.9
183	10/08/1992	22:12:19.42	1.6	38.290	15.997	15.45	11	105	0.08	0.6	1.1
184	12/08/1992	03:36:52.20	0.7	38.343	16.081	9.87	8	106	0.04	0.9	2.1
185	11/09/1992	12:05:31.43	2.2	38.280	16.029	12.28	11	135	0.09	0.8	1.2
186	11/09/1992	21:16:48.29	1.3	38.273	16.033	12.59	8	160	0.07	0.8	1.4
187	11/09/1992	21:30:43.36	2.1	38.262	16.04	15.39	12	220	0.07	0.6	0.8
188	11/09/1992	21:34:12.69	1.5	38.259	16.038	12.8	12	203	0.13	0.6	0.8
189	11/09/1992	21:36:46.91	2.0	38.265	16.043	13.54	11	218	0.08	0.8	0.8
190	11/09/1992	21:40:37.08	1.7	38.266	16.034	12.5	10	205	0.1	0.8	1.3
191	11/09/1992	21:44:12.83	1.6	38.264	16.039	14.47	9	208	0.06	0.9	1.3
192	11/09/1992	21:54:18.75	1.0	38.267	16.036	13.98	7	198	0.08	1	1.7
193	11/09/1992	21:59:09.57	1.1	38.270	16.042	16.61	10	195	0.14	0.6	1
194	11/09/1992	22:00:38.98	2.1	38.276	16.029	12.04	11	139	0.09	0.8	1.2
195	11/09/1992	22:01:23.17	1.6	38.261	16.038	14.16	10	221	0.07	0.9	1.3
196	11/09/1992	22:25:24.05	1.5	38.262	16.038	14.53	9	219	0.06	0.9	1.3
197	11/09/1992	22:53:51.68	1.1	38.268	16.04	13.65	9	204	0.07	0.8	0.9
198	11/09/1992	23:00:46.96	0.7	38.319	16.016	1.86	7	97	0.21	0.9	1.4
199	11/09/1992	23:58:05.50	1.0	38.280	16.028	11.18	7	132	0.07	1.4	2.3
200	12/09/1992	00:02:07.72	1.0	38.262	16.041	14.91	9	221	0.07	0.9	1.3
201	12/09/1992	00:09:17.40	0.8	38.263	16.04	13.29	9	219	0.09	0.4	0.8
202	12/09/1992	00:48:10.56	0.5	38.319	16.015	1.83	6	134	0.22	0.9	1.6
203	12/09/1992	01:58:10.93	1.0	38.280	16.028	10.81	8	131	0.07	1.2	1.6
204	12/09/1992	03:03:25.90	0.9	38.268	16.036	13.1	7	196	0.06	1	1.7
205	12/09/1992	03:29:06.56	1.1	38.267	16.044	12.48	10	211	0.09	0.8	0.7
206	12/09/1992	04:27:17.23	1.3	38.270	16.043	12.28	9	198	0.09	0.8	0.7
207	12/09/1992	05:37:42.28	1.2	38.261	16.037	14.29	9	220	0.07	0.9	1.3
208	12/09/1992	05:38:21.74	1.2	38.320	16.02	0.01	7	97	0.25	0.7	2.5
209	12/09/1992	05:38:36.19	1.4	38.258	16.038	14.48	9	223	0.07	0.9	1.3
210	12/09/1992	06:15:30.92	0.9	38.316	16.025	0.85	6	101	0.21	0.4	3
211	12/09/1992	06:35:34.98	1.1	38.319	16.019	0.05	7	97	0.24	0.7	2.3
212	12/09/1992	07:22:15.96	0.8	38.320	16.019	0.01	7	97	0.25	0.8	2.7
213	12/09/1992	10:02:11.58	0.8	38.270	16.04	14.14	6	195	0.06	1.1	1.6
214	18/09/1992	01:23:12.64	1.5	38.272	16.031	12.55	10	155	0.07	0.8	1.3
215	18/09/1992	03:56:35.45	1.0	38.269	16.034	13.22	8	183	0.05	0.9	1.4

Table I. (*continued*).

N°	Date	Orig. Time	M_L	Lat. N°	Long. E°	Depth	N	Gap	rms	Erh	Erz
216	18/09/1992	04:48:24.98	1.5	38.273	16.032	12.56	9	157	0.06	0.8	1.3
217	19/09/1992	14:31:17.14	1.2	38.317	16.051	15.38	8	124	0.04	0.8	1.4
218	29/10/1992	21:16:32.60	1.3	38.382	16.14	14.76	10	187	0.05	0.7	1.3
219	11/11/1992	04:48:34.60	1.0	38.502	15.958	13.22	6	133	0.03	1	2
220	04/12/1992	19:32:02.12	0.5	38.440	16.014	11.55	6	174	0.06	1.3	3
221	07/12/1992	04:06:00.46	1.5	38.272	16.031	14.58	10	156	0.1	0.7	0.8
222	16/01/1993	13:20:39.96	0.5	38.275	16.013	12.82	6	118	0.05	1.2	2.1
223	06/03/1993	09:07:16.22	2.2	38.416	16.201	15.27	8	248	0.06	0.9	1.5
224	10/04/1993	20:50:10.97	1.9	38.337	16.12	17.11	11	117	0.07	0.7	1.2
225	23/04/1993	02:46:32.05	1.0	38.438	15.919	12.98	10	152	0.1	0.8	1.4
226	11/05/1993	06:36:07.15	1.2	38.302	15.932	16.31	10	88	0.09	0.8	1.1
227	02/06/1993	08:26:14.41	2.1	38.535	16.053	17.35	10	174	0.06	0.6	1.4
228	24/06/1993	05:50:10.83	1.3	38.313	16.023	16.13	6	138	0.03	0.9	1.6
229	30/06/1993	21:20:27.01	2.0	38.342	15.94	16.46	10	105	0.09	0.6	1.2
230	30/06/1993	22:07:50.91	1.8	38.339	15.938	16.94	9	133	0.09	0.7	1.2
231	30/06/1993	23:49:35.53	0.7	38.345	15.934	16.88	6	144	0.05	1.1	1.6
232	01/07/1993	18:52:19.12	1.1	38.343	15.937	16.91	7	147	0.05	1.1	1.6
233	01/07/1993	19:01:49.32	2.1	38.343	15.938	16.49	11	81	0.08	0.6	1.2
234	01/07/1993	19:43:11.91	1.1	38.342	15.937	16.96	9	104	0.06	0.9	1.4
235	01/07/1993	20:29:50.40	1.1	38.341	15.936	17.02	7	149	0.06	1.1	1.6
236	01/07/1993	20:34:56.45	1.3	38.341	15.941	17.82	8	150	0.04	0.6	1.5
237	01/07/1993	21:06:47.01	1.4	38.337	15.939	17.36	10	155	0.09	1	1.5
238	01/07/1993	21:41:53.12	1.4	38.343	15.94	16.41	11	79	0.08	0.6	1.2
239	01/07/1993	22:55:17.24	1.5	38.337	15.94	17.41	10	155	0.08	1	1.5
240	02/07/1993	00:18:23.24	1.3	38.347	15.946	15.78	11	105	0.1	0.6	1.2
241	02/07/1993	00:20:12.80	1.1	38.335	15.933	17.52	8	154	0.08	1	1.5
242	02/07/1993	01:03:54.61	1.9	38.344	15.941	16.53	12	79	0.09	0.6	1.2
243	02/07/1993	04:16:11.71	1.3	38.346	15.942	16.42	9	132	0.07	0.7	1.2
244	02/07/1993	12:40:16.91	0.9	38.364	15.974	0.45	6	134	0.19	0.4	3
245	02/07/1993	13:55:44.29	1.1	38.363	15.975	0.09	6	136	0.17	0.5	1.5
246	02/07/1993	16:17:51.98	1.5	38.326	16.018	11.92	10	89	0.05	0.5	1.3
247	15/07/1993	10:18:04.47	2.0	38.452	16.11	14.21	10	138	0.07	0.6	1.2
248	12/08/1993	01:03:41.90	0.5	38.275	16.035	12.79	6	161	0.04	1.3	1.9
249	13/08/1993	20:54:21.18	0.6	38.276	16.035	12.51	8	161	0.08	0.8	1.4
250	13/09/1993	11:51:20.14	0.9	38.299	16.04	16.04	8	133	0.19	0.8	1.4
251	18/12/1993	06:53:57.30	1.9	38.432	15.941	16.42	10	115	0.12	0.5	0.8
252	13/03/1994	14:02:49.43	2.8	38.450	15.891	43.59	10	199	0.1	1.5	1.4

(1935) procedure (Di Grazia *et al*., 2001). The estimated M_L ranges between 0.5 and 3.0.

3. Data analysis and results

3.1. *Focal mechanisms and stress tensor analysis*

Fault plane solutions (FPS) were determined using the FPFIT program (Reasenberg and Oppenheimer, 1985). The FPFIT program constrains the mechanism to be double-couple and performs a grid search over the available solution space. In order to obtain good azimuthal data coverage for each focal mechanism solution, seismograms were reread to check polarities and a minimum of 7 impulsive P-wave first motions in different azimuth (9 on average) were considered for each selected event. The final dataset consists of 120 well-constrained fault plane solutions (figs. 2 and 3; table II). In particular, 53% normal faulting, 46% strike slip faulting, and 2% reverse faulting mechanisms have been identified. The FPFIT program output also gives P- and T- axes orientation. The spatial distribution of deformation axes (fig. 2) shows for the P-axes a strong dispersion with a maximum in the N40°-60°E class. Conversely, the prevalence of the T-axes in the N300°-320°E is well evidenced.

To determine stress directions from fault plane solutions, we used the Focal Mechanism Stress Inversion (FMSI) computer program developed by Gephart and Forsyth (1984) and Gephart (1990). This method is based on the following basic assumptions: 1) stress is uniform in the rock volume of the seismic sample investigated; 2) earthquakes are shear dislocations on pre-existing faults; 3) slip occurs in the direction of the resolved shear stress on the fault plane. Four stress parameters are calculated: three of them define the orientations of the main stress axes σ_1, σ_2, and σ_3, the other is a measure of relative stress magnitude $R=(\sigma_2-\sigma_1)/(\sigma_3-\sigma_1)$. Moreover, a variable misfit (F) is introduced to define discrepancies between the stress tensor and the observed fault plane solutions. For a given stress model, the misfit of a single focal mechanism is defined as the smallest rotation around any arbitrary axis which brings one of the nodal planes, its slip direction and the sense of slip into an orientation that is consistent with the stress model. Each FPS receives two misfits, one for each nodal plane. If an *a priori* choice of the fault plane is not made, the nodal plane with the smallest misfit is assumed as the fault plane. The size of the average misfit provides a guide of how well the assumption of stress homogeneity is fulfilled in relation to the seismic sample submitted to the inversion algorithm (Michael, 1987). In the light of the results from a series of tests carried out by Wyss *et al*. (1992), Gillard *et al*. (1996), Cocina *et al*. (1997) to identify the relationship between FPS uncertainties and average misfit in the case of uniform stress, we assume that the condition of a homogeneous stress distribution is fulfilled if the misfit, F, is smaller than 6° and that it is not fulfilled if F>9°. For F values between 6° and 9° the solution is considered acceptable, but it may reflect some heterogeneity. The statistical confidence limits established for possible stress orientations that are consistent with the observed focal mechanisms may give an additional contribution because they generally tend to enlarge for increasing stress heterogeneity (Cocina *et al*., 1997). We computed the 90% confidence level using the statistical procedure described by Parker and McNutt (1980) and Gephart and Forsyth (1984). The size of the 90% confidence limits will not be a criterion for preferring an inversion result, because it does not measure the quality of the result but rather the degree to which it is constrained.

In the present study, the Gephart and Forsyth (1984) inversion algorithm was applied to the 120 well-constrained fault plane solutions. If they are produced by a single stress tensor, then the variety among the fault plane solutions may be the result of the presence of planes of weakness with different orientations to accommodate the slip. On the other hand, the variation could reflect the inhomogeneity of stress within the crust.

Each of the FPS was assigned a weight (1=sufficiently constrained, 2=well constrained) based on a qualitative evaluation of the polarity distribution and score. Fault parameter uncer-

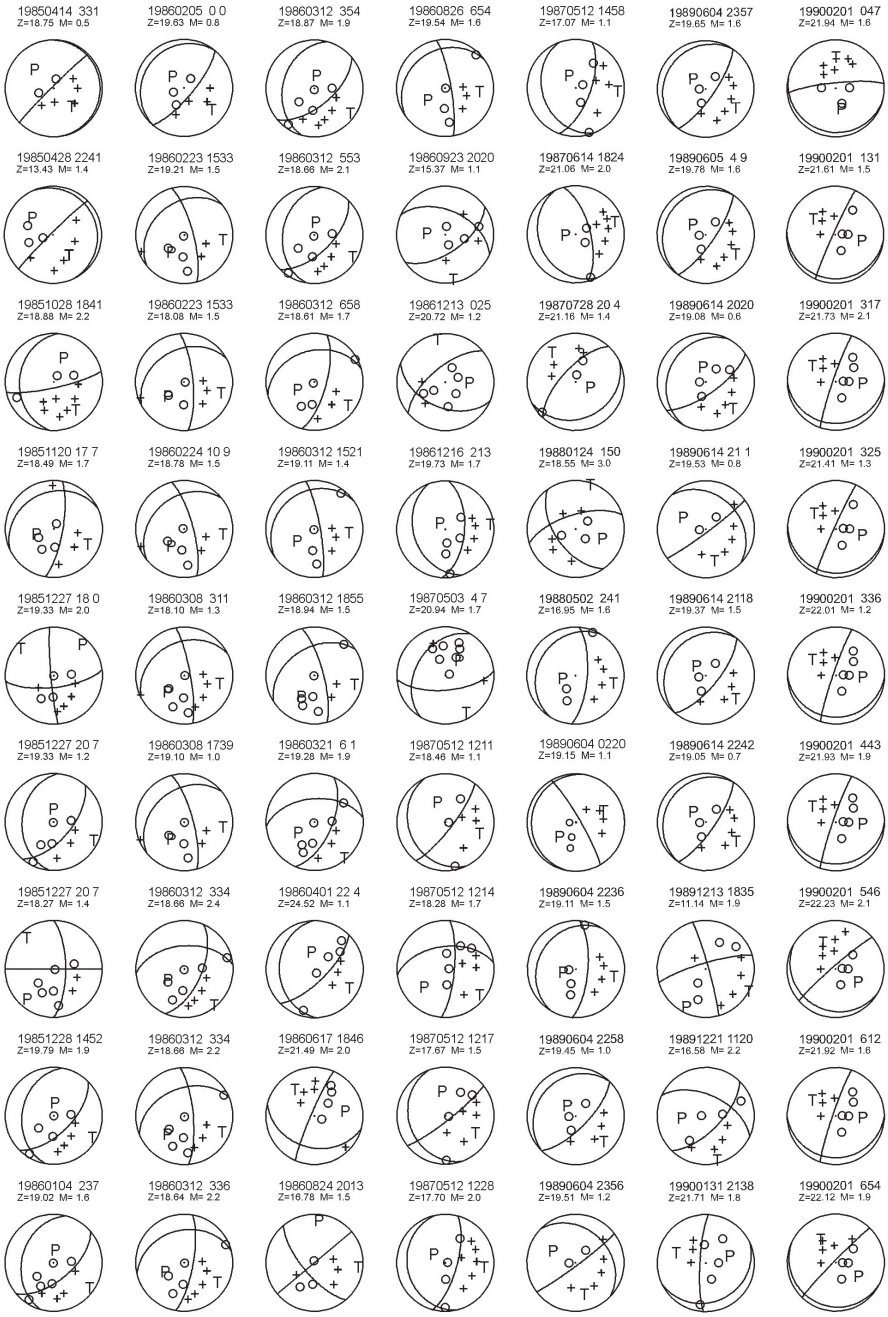

Fig. 2. Fault plane solutions (lower hemisphere equal-area projection) of the 120 best constrained events. For each mechanism the date (year, month, day), the origin time (hour, minute), the focal depth in km (z) and the magnitude (M_L) are reported. P and T denote the P- and T-axes position. Open circles and crosses indicate dilatations and compressions, respectively.

Fig. 2. (*continued*)

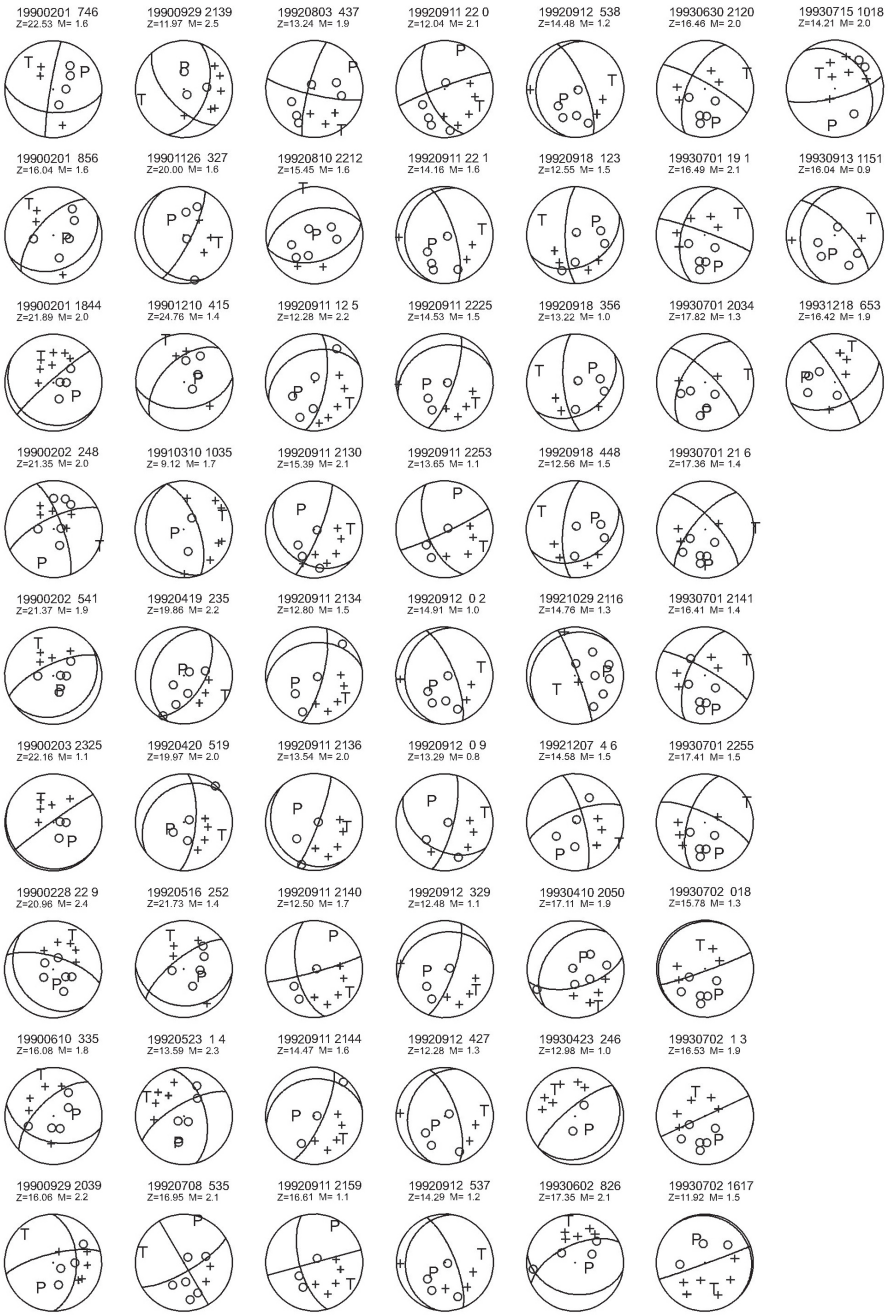

Table II. Focal parameters of the 120 selected events. Strike, Dip, Rake, Azimuth and Plunge are given in degrees. Δ is the error referred to the nodal plane.

										Paxis		Taxis	
N°	**Date**	**Orig. Time**	**N_p**	**Strike**	**Dip**	**Rake**	**ΔStr**	**ΔDip**	**ΔRake**	**Azm**	**Plunge**	**Azm**	**Plunge**
1	14/04/1985	03:31:22.04	7	355	5	40	15	10	15	311	42	139	48
4	28/04/1985	22:41:03.14	8	335	10	20	13	13	10	306	41	145	48
12	28/10/1985	18:41:47.79	10	185	30	-160	13	10	10	17	47	145	29
14	20/11/1985	17:07:22.24	8	10	75	-110	10	10	20	255	56	116	27
18	27/12/1985	18:00:10.63	9	175	85	-160	3	3	10	41	18	307	10
20	27/12/1985	20:07:31.85	8	185	35	-120	20	10	10	350	69	116	13
21	27/12/1985	20:07:49.31	8	270	90	-20	5	10	10	223	14	317	14
22	28/12/1985	14:52:24.25	9	190	35	-120	20	10	10	355	69	121	13
24	04/01/1986	02:37:06.54	10	195	35	-120	20	8	10	360	69	126	13
27	05/02/1986	00:00:30.34	7	40	75	-90	13	5	20	310	60	130	30
28	23/02/1986	15:33:29.42	7	345	75	-120	10	10	20	221	51	98	24
29	23/02/1986	15:33:47.76	7	355	75	-120	20	13	20	231	51	108	24
31	24/02/1986	10:09:56.51	7	345	75	-120	10	10	20	221	51	98	24
32	08/03/1986	03:11:28.64	10	350	80	-120	5	8	20	229	47	104	29
33	08/03/1986	17:39:09.65	7	345	75	-120	13	10	20	221	51	98	24
34	12/03/1986	03:34:09.64	10	265	50	-40	10	20	10	240	53	142	6
35	12/03/1986	03:34:13.93	9	355	75	-130	3	8	20	225	45	114	20
36	12/03/1986	03:36:04.43	10	10	75	-120	8	10	20	246	51	123	24
38	12/03/1986	03:54:00.19	10	195	35	-120	18	8	10	360	69	126	13
41	12/03/1986	05:53:25.81	9	190	35	-120	18	10	10	355	69	121	13
42	12/03/1986	06:58:59.54	7	15	70	-120	13	13	20	247	55	127	19
44	12/03/1986	15:21:38.95	7	350	80	-110	20	13	20	237	51	97	32
45	12/03/1986	18:55:09.54	8	345	75	-130	13	10	20	215	45	104	20
46	21/03/1986	06:01:18.65	9	265	50	-40	13	20	10	240	53	142	6
47	01/04/1986	22:04:28.45	8	45	70	-70	5	5	20	344	60	120	22
49	17/06/1986	18:46:00.44	9	105	35	-10	10	20	20	81	41	321	31
57	24/08/1986	20:13:25.54	7	140	70	-180	10	13	5	3	14	97	14
58	26/08/1986	06:54:18.47	7	350	80	-110	20	10	20	237	51	97	32
60	23/09/1986	20:20:35.27	7	55	60	-130	5	5	10	272	55	172	7
65	13/12/1986	00:25:35.03	8	230	65	-130	10	13	5	92	52	348	11
67	16/12/1986	02:13:16.01	9	160	35	-110	10	10	20	310	74	84	11
72	03/05/1987	04:07:40.12	8	85	65	-60	20	5	5	38	59	154	15
75	12/05/1987	12:11:15.13	7	155	25	-150	13	20	15	333	52	110	29
77	12/05/1987	12:14:59.85	9	5	75	-140	18	8	10	231	38	129	15

Table II. (*continued*).

										Paxis		Taxis	
N°	**Date**	**Orig. Time**	**N_p**	**Strike**	**Dip**	**Rake**	**ΔStr**	**ΔDip**	**ΔRake**	**Azm**	**Plunge**	**Azm**	**Plunge**
78	12/05/1987	12:17:39.33	9	160	25	-160	3	10	5	347	48	122	33
80	12/05/1987	12:28:38.11	10	15	70	-80	8	0	20	301	64	97	24
81	12/05/1987	14:58:19.51	8	20	65	-70	8	3	20	324	64	95	18
84	14/06/1987	18:24:08.19	9	155	25	-100	20	5	20	265	69	73	20
85	28/07/1987	20:04:14.44	7	65	25	-70	10	5	10	116	67	320	21
90	24/01/1988	01:50:50.12	8	145	55	-30	20	5	10	113	44	17	7
96	02/05/1988	02:41:02.81	7	5	70	-100	20	13	20	259	64	103	24
111	04/06/1989	02:20:47.67	7	190	10	-50	20	20	20	234	48	70	38
112	04/06/1989	22:36:21.41	8	5	70	-100	18	10	20	259	64	103	24
113	04/06/1989	22:58:02.94	7	45	70	-90	13	5	20	315	65	135	25
114	04/06/1989	23:56:18.07	7	315	30	-10	20	10	10	295	42	168	33
115	04/06/1989	23:57:03.76	9	35	75	-90	8	5	20	305	60	125	30
116	05/06/1989	04:09:21.01	9	35	75	-90	8	5	20	305	60	125	30
118	14/06/1989	20:20:22.97	9	55	70	-80	8	3	20	341	64	137	24
119	14/06/1989	21:01:00.28	7	315	30	-10	20	10	10	295	42	168	33
120	14/06/1989	21:18:58.92	7	40	70	-90	13	5	20	310	65	130	25
121	14/06/1989	22:42:35.30	8	35	75	-90	8	5	20	305	60	125	30
128	13/12/1989	18:35:49.30	9	345	85	-170	3	13	20	210	11	119	3
130	21/12/1989	11:20:23.95	8	45	65	-140	8	5	10	265	45	168	6
134	31/01/1990	21:38:17.50	8	65	20	-30	18	18	20	73	52	288	33
136	01/02/1990	00:47:27.58	9	105	10	-70	20	10	20	171	54	358	36
137	01/02/1990	01:31:18.08	8	95	10	-20	20	20	20	105	48	304	41
138	01/02/1990	03:17:57.13	9	90	15	-20	20	20	20	94	48	302	38
139	01/02/1990	03:25:16.57	8	95	10	-20	20	20	20	105	48	304	41
140	01/02/1990	03:36:09.93	9	90	15	-20	20	20	20	94	48	302	38
141	01/02/1990	04:43:30.58	9	90	15	-20	20	20	20	94	48	302	38
144	01/02/1990	05:46:02.16	10	120	15	-20	10	15	10	124	48	332	38
145	01/02/1990	06:12:50.19	9	90	15	-20	20	20	20	94	48	302	38
146	01/02/1990	06:54:18.82	9	115	10	-20	10	20	10	125	48	324	41
147	01/02/1990	07:46:38.53	7	190	85	-140	20	15	10	61	31	316	23
148	01/02/1990	08:56:54.99	8	65	30	-70	10	8	10	108	71	320	16
149	01/02/1990	18:44:58.38	11	120	15	-20	8	20	10	124	48	332	38
150	02/02/1990	02:48:35.13	11	340	75	-160	15	3	0	203	25	112	3

Table II. (*continued*).

										Paxis		Taxis	
N°	**Date**	**Orig. Time**	**N_p**	**Strike**	**Dip**	**Rake**	**ΔStr**	**ΔDip**	**ΔRake**	**Azm**	**Plunge**	**Azm**	**Plunge**
151	02/02/1990	05:41:31.89	9	55	20	-100	10	8	10	162	65	333	25
155	03/02/1990	23:25:23.83	8	115	5	-30	20	20	15	140	47	329	42
158	28/02/1990	22:09:46.68	11	140	25	-60	10	8	10	176	64	28	22
161	10/06/1990	03:35:05.70	10	105	45	-40	10	13	20	87	55	342	10
163	29/09/1990	20:39:35.05	9	0	50	-160	3	3	0	210	40	314	16
164	29/09/1990	21:39:11.39	9	20	50	-40	18	5	10	355	53	257	6
166	26/11/1990	03:27:20.77	7	155	20	-140	8	8	15	316	55	104	31
167	10/12/1990	04:15:15.48	7	85	45	-60	13	5	15	74	69	334	4
169	10/03/1991	10:35:10.98	9	160	25	-90	20	5	10	250	70	70	20
175	19/04/1992	02:35:55.35	9	200	35	-100	20	10	20	327	78	117	10
176	20/04/1992	05:19:12.00	8	5	70	-110	15	13	20	246	60	110	22
178	16/05/1992	02:52:56.20	9	95	25	-50	8	5	5	118	60	335	24
179	23/05/1992	01:04:56.21	10	240	70	-40	10	13	10	197	42	297	11
180	08/07/1992	05:35:54.28	8	60	75	0	5	5	5	16	11	284	11
182	03/08/1992	04:37:14.52	9	195	80	-170	5	10	20	59	14	149	0
183	10/08/1992	22:12:19.42	8	75	45	-90	18	8	20	241	90	345	0
185	11/09/1992	12:05:31.43	10	10	70	-120	10	15	20	242	55	122	19
187	11/09/1992	21:30:43.36	10	130	30	-160	5	5	0	322	47	90	29
188	11/09/1992	21:34:12.69	9	15	75	-120	3	5	20	251	51	128	24
189	11/09/1992	21:36:46.91	8	140	15	-150	10	10	10	305	51	99	36
190	11/09/1992	21:40:37.08	8	75	85	-30	10	3	10	27	24	125	17
191	11/09/1992	21:44:12.83	8	25	75	-110	10	8	20	270	56	131	27
193	11/09/1992	21:59:09.57	8	165	65	-180	5	10	0	27	17	123	17
194	11/09/1992	22:00:38.98	10	250	85	30	8	5	5	20	17	118	24
195	11/09/1992	22:01:23.17	8	195	20	-60	18	10	10	238	61	82	27
196	11/09/1992	22:25:24.05	8	20	75	-110	13	8	20	265	56	126	27
197	11/09/1992	22:53:51.68	7	65	85	-30	10	5	5	17	24	115	17
200	12/09/1992	00:02:07.72	8	190	20	-60	18	10	10	233	61	77	27
201	12/09/1992	00:09:17.40	7	15	75	-50	13	8	5	325	45	76	20
205	12/09/1992	03:29:06.56	8	20	75	-110	10	5	20	265	56	126	27
206	12/09/1992	04:27:17.23	7	195	25	-60	18	10	10	231	64	83	22
207	12/09/1992	05:37:42.28	8	190	20	-60	18	13	20	233	61	77	27
208	12/09/1992	05:38:21.74	8	190	20	-60	18	10	10	233	61	77	27

Table II. (*continued*).

										Paxis		Taxis	
N°	**Date**	**Orig. Time**	**N_p**	**Strike**	**Dip**	**Rake**	**ΔStr**	**ΔDip**	**ΔRake**	**Azm**	**Plunge**	**Azm**	**Plunge**
215	18/09/1992	03:56:35.45	7	175	70	-120	15	5	5	47	55	287	19
216	18/09/1992	04:48:24.98	8	185	70	-120	15	13	10	57	55	297	19
218	29/10/1992	21:16:32.60	9	230	15	160	8	18	10	82	38	234	48
221	07/12/1992	04:06:00.46	7	345	75	-160	20	15	10	208	25	117	3
224	10/04/1993	20:50:10.97	10	75	60	-70	10	8	20	26	68	151	13
225	23/04/1993	02:46:32.05	8	50	15	-90	20	10	20	140	60	320	30
227	02/06/1993	08:26:14.41	9	100	35	-60	10	8	10	115	69	349	13
229	30/06/1993	21:20:27.01	9	300	80	-150	15	15	10	166	28	69	13
233	01/07/1993	19:01:49.32	10	290	85	-140	10	8	0	161	31	56	23
236	01/07/1993	20:34:56.45	7	315	75	-140	10	10	5	181	38	79	15
237	01/07/1993	21:06:47.01	9	220	70	-20	10	10	10	179	28	88	1
238	01/07/1993	21:41:53.12	10	300	80	-150	10	8	5	166	28	69	13
239	01/07/1993	22:55:17.24	9	295	75	-150	8	8	5	159	32	63	9
240	02/07/1993	00:18:23.24	10	210	5	50	5	8	5	157	41	344	49
242	02/07/1993	01:03:54.61	11	65	90	90	3	5	10	155	45	335	45
246	02/07/1993	16:17:51.98	9	320	5	-20	10	20	20	335	47	164	43
247	15/07/1993	10:18:04.47	9	75	75	60	8	3	10	188	24	311	51
250	13/09/1993	11:51:20.14	7	190	30	-40	18	13	20	194	57	64	23
251	18/12/1993	06:53:57.30	8	65	50	-170	20	8	10	279	33	23	21

tainties range between 5 and 20 degrees, with the great majority of cases between 10 and 15 degrees. The initial inversion consisted of a search of the entire range of possible stress orientations on a 10-degree grid using the approximate method. The regions of possible solutions suggested by the approximate method were then searched more thoroughly using the exact method on a 5-degree grid. The ratio R was searched at intervals of 0.1.

First, the entire dataset of focal mechanisms was inverted. The inversion led us to find an approximately NE-SW vertical σ_1 and horizontal σ_2 and σ_3 (fig. 3a and table III, dataset a). The stress ratio value (R=0.7) indicates an almost uniaxial deviatoric compression. The average misfit for this inversion is 6.2. This value suggests that this dataset may be slightly contaminated by heterogeneity.

In order to test the stability of the results in this region, we also performed a second stress inversion by following both the criteria of homogeneity in the dataset (*i.e.* fault plane solution categories and P- and T-axes orientation) and the structural-geological setting of the area. Therefore, the dataset of focal mechanisms was divided into two subsets (fig. 3b,c and table III, datasets b and c) as a function of space based on the pattern of seismicity distribution along the surface geologic structure NE-SW trending of Cittanova normal fault system.

For each subset several tests were performed using different grid steps and a large variety of starting values for the stress parame-

ters in order to check the reliability of the results. For the first investigated sub volume (along the CF, dataset b in table III and fig. 3b), we inverted 83 focal mechanisms obtaining an average misfit of 5.6. The previously described indication of a NW-SE extension in this part of the belt is confirmed. The inversion of the remaining 37 events, located westward and northwestward of CF, gives again a horizontal σ_3, oriented approximately WNW-ESE, and a ver-

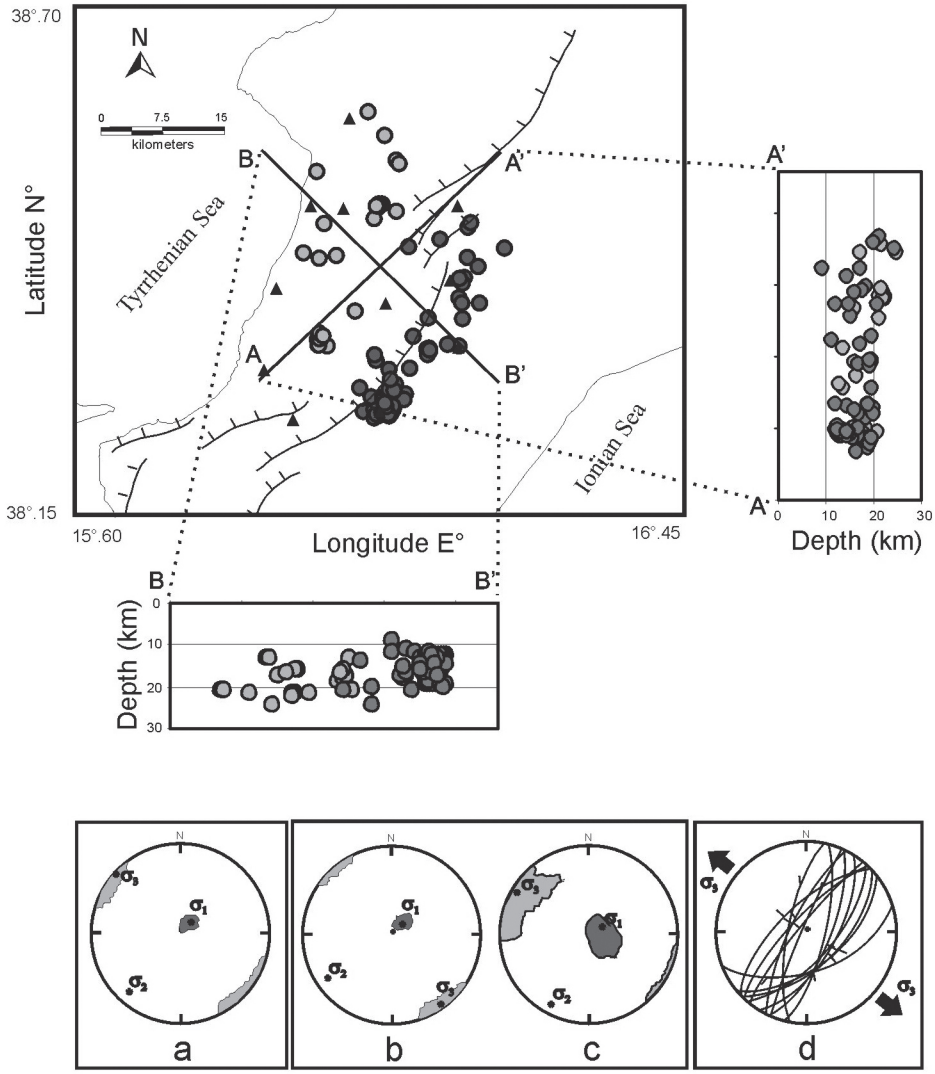

Fig. 3a-d. Map and SW-NE (A-A') and NW-SE (B-B') cross sections of the earthquakes selected for stress tensor inversion. Lower-hemisphere projection of the orientations (stars) of the principal stress axes obtained by inverting the whole dataset (a) and the two different subsets (b) and (c). Gray areas indicate the 90% confidence limits of σ_1 and σ_3 orientations. d) Diagram (Schmidt net, lower hemisphere) showing fault planes and slickensides measured along cataclastic belts of Cittanova fault. Large arrows indicate azimuth of the mean extension direction derived from a qualitative and quantitative analysis of the slickenside data sets (Tortorici *et al*., 1995).

tical σ_1 (dataset c in table III and fig. 3c). The average misfit is 6.0° which is the limit for acceptable results and may indicate that this dataset is not completely homogeneous.

Table III. Results from Stress Inversion Runs. N, F and R are, respectively, the number of events, the average misfit corresponding to the stress solution found and the measure of relative stress magnitude. Deviatoric principal stress axes, σ_1, σ_2, σ_3, are the compressional, intermediate and extensional deviatoric axes, respectively. They are specified by plunges measured from horizontal and azimuth measured clockwise from north. For the corresponding dataset, see the text.

Dataset	N	F (°)	σ_1		σ_2		σ_3		R
			Pl(°)	Az(°)	Pl(°)	Az(°)	Pl(°)	Az(°)	
a	120	6.2	76	45	14	222	1	312	0.7
b	83	5.6	76	45	14	236	3	145	0.8
c	37	6.0	76	65	11	209	8	300	0.8

3.2 *Evaluation of Q_P*

The method here used for Q_P estimate is based on the time domain formulation deriving from the classic rise time (or pulse-broadening) method (*e.g.* Gladwin and Stacey, 1974; Wu and Lees, 1996). It is based on the measure of the first P pulse width τ in time domain, under the assumption that the quality factor Q is frequency-independent. The pulse width τ, for velocity records, can be defined as the time difference from the onset to the first zero crossing (fig. 4). For point-like impulsive sources it is expressed by the linear relation:

$$\tau = \tau_0 + CT / Q_p \qquad (3.1)$$

where τ_0 is the original pulse width at the source, T is the travel time, Q_P is the quality factor of P-waves and C is a constant which is equal to 0.5 for a constant Q attenuation operator (Kjartansson, 1979). The linear relation between τ and T/Q_P predicted by equation (3.1) holds for point-like sources. In fact, the only limiting assumption of this method is that it neglects the directivity effect of the seismic radiation generated by a finite dimension seismic source (Zollo and de Lorenzo, 2001).

The rise time method is expected to give more reliable estimates of the intrinsic attenuation than spectral techniques for several reasons. First, the rise time is not affected by non-objective criteria of phase windowing; second, since only a very limited portion of the seismogram is used, the effects of secondary arrivals due to waves diffracted by heterogeneities in the medium and site effects are minimized. Moreover, since the rise time method does not use wave amplitudes, correction for the instrumental response is not needed provided that the latter is flat in the dominant frequency range of the earthquakes (*e.g.* Zollo and de Lorenzo, 2001). However, to take full advantage of this method it is essential that the shape of the pulse to be used is not greatly distorted by the seismogram. Therefore, the most reliable results will be obtained using signals recorded with a high signal-to-noise ratio. Following this criterion, from the entire dataset shown in fig. 1 and table I, we selected 110 earthquakes with magnitude ranging between 1.0 and 3.0 and depth ranging between 10 and 25 km. A total of 607 waveforms with clear P-wave onset, high signal-to-noise ratio and not affected by multipathing during the first half-cycle of the wave, were considered suitable for the application of the rise time method. We did not perform the correction for the instrumental response because the filtering operated in the deconvolution can generate artificial signals (Mulargia and Geller, 2003 and references therein). Moreover, since the frequency content of first pulses is always contained in the range where the response of the instruments is flat, rise times should be un-

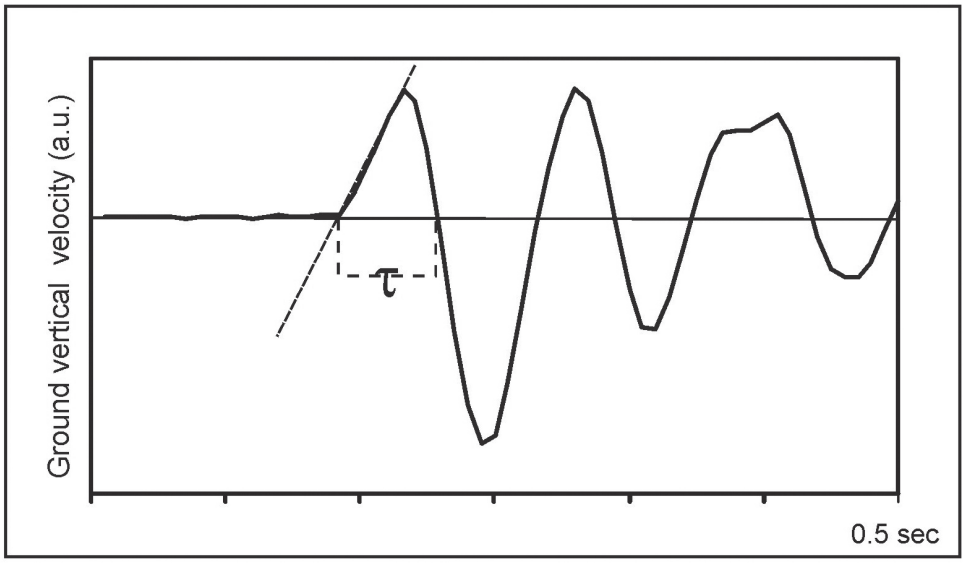

Fig. 4. Schematic picture of rise time as measured on a velocity seismogram.

affected by instrumental effects. The rise time of P-waves was measured on each vertical seismogram using a semi-automatic procedure which computes the time interval between the onset of the P-wave and its first zero crossing.

We first plotted all τ values vs. travel time (T) considering the minimum 1D velocity model proposed by Raffaele *et al*. (2006). A first observation consists of the positive trend of rise times vs. the travelled distances, even though some scatter in the data is observed (fig. 5). The dispersion of the data around the line of best fit may be due either to spatial variations in the attenuation properties of the ray sampled volume and/or to directivity source effects. Under the simplified assumption of a non-directive source we obtained an average estimate of Q_P as 84±8. Then, in order to estimate the intrinsic attenuation at each station site and to evidence possible lateral variations in the anelastic properties of the medium, we plotted τ values vs. T for each station. Table IV reports the inferred estimates of Q_P at 10 stations (we did not include GTSM station because of the low number of data available), together with the relative standard deviation. The Q_P values obtained at most of the stations are, within the error, very close to the average Q_P obtained for the whole area. However, lower Q_P values are obtained at stations DLV and ZMR and higher Q_P are found at stations CCL and STC.

Finally, we plotted τ values vs. T for each event and computed the best fit straight line. Some of these fits are reported, as examples, in fig. 6. The events for which the slope of the

Table IV. Q_P values and relative errors at each seismic station.

Station Name	$Q_P \pm \sigma$
CCL	100±24
CGT	56±16
CLT	86±30
CSB	77±19
CST	54±15
DLV	38±9
MTR	78±20
PDL	68±17
STC	149±53
ZMR	36±4

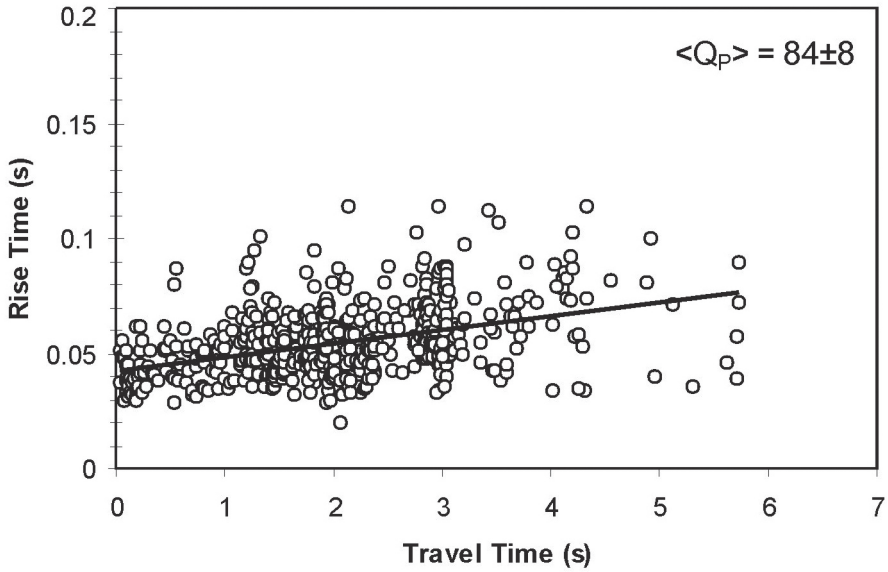

Fig. 5. Rise time plotted as a function of travel time. The best fit interpolating straight line is also shown.

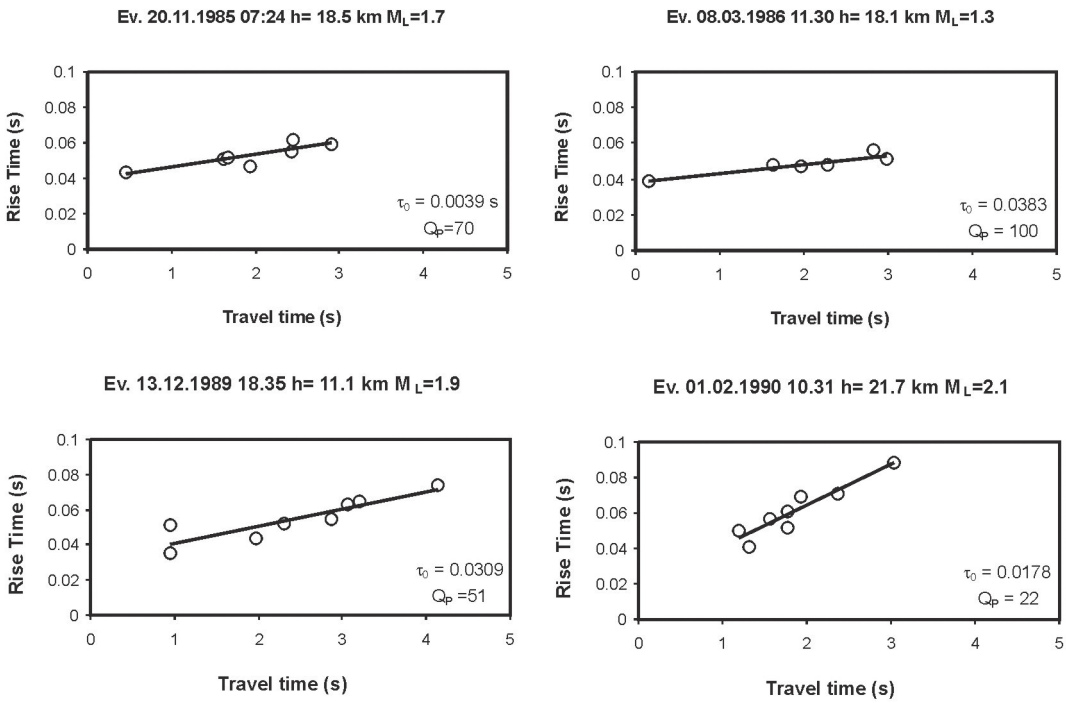

Fig. 6. Rise time vs. travel time for some events considered in this study. The best fitting straight line is also shown.

straight line described by equation (3.1) was negative have no physical significance and were discarded. A total of 89 events were considered. We obtained, for each event, a Q_P value ranging between 14 and 400 and an average Q_P =87, which is very close to the average value obtained from the linear regression of the whole dataset.

3.3. *Source parameters estimate*

For a circular crack, the source rise time, which represents the time duration of the slipping on the fault, is related to the source radius L and the rupture velocity (Boatwright, 1980). We used the source rise times τ_0 calculated for each of the 89 events to estimate the source dimension L by using the following relationship:

$$\tau_0 = L / V_r \qquad (3.2)$$

where V_r is the average rupture velocity here assumed equal to 0.9 V_S, with V_S the average S-wave velocity. Considering the average V_S =3.6 km/s (Raffaele *et al*., 2006), the used V_r is 3.24 km/s. We obtained source radii varying from a few meters to 200 m (table V).

For each event the seismic moment M_0 was calculated from the estimated local magnitude M_L (table V) by using the general empirical relationship by Bakun and Lindth (1977):

$$\text{Log } M_0 = 1.2\ M_L + 17 \qquad (3.3)$$

The estimated M_0 values were plotted vs. source dimension in fig. 7a. The lines of constant stress drop $\Delta\sigma$ were obtained by using the scaling relationship for circular earthquake sources (Keilis-Borok, 1959):

$$\Delta\sigma = \frac{7M_0}{16L^3} \qquad (3.4)$$

The stress drop of most of the events is low and concentrated between 0.1 and 10 bars, with an average value around 5 bars. Only few events have higher stress drop, up to 100 bars (figs. 7a,b and 8; table V). It must be stressed that according to equation (3.2), source radius estimates, and therefore stress drop, are rupture velocity-dependent (*e.g*. Zollo and de Lorenzo, 2001). The average rupture velocity of small magnitude events is usually poorly known. Theoretical and laboratory studies (Madariaga, 1976) indicate that V_r varies between 0.6 V_S and

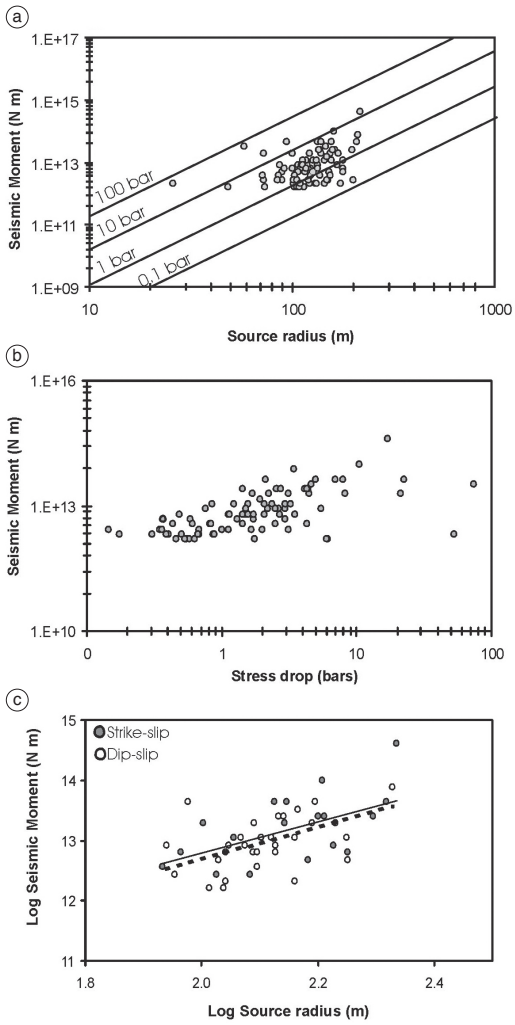

Fig. 7a-c. a) Seismic moment vs. source dimensions. The lines of constant stress drop are also reported. b) Seismic moment vs. stress drop. c) Scaling relations seismic moment-source radius for dip-slip (black line) and strike-slip (black dotted line) source mechanisms.

Table V. Source parameters of the analysed events.

N°	Date	Orig. Time	M_L	L (m)	M_0 (N m)	$\Delta\sigma$ (bars)
4	28/04/1985	22:41:03.14	1.4	178	4.79E+12	0.37
8	24/08/1985	17:56:37.65	1	73	1.58E+12	1.77
10	26/10/1985	16:52:03.04	1.2	151	2.75E+12	0.35
11	27/10/1985	06:44:54.88	1.5	101	6.31E+12	2.72
12	28/10/1985	18:41:47.79	2.2	134	4.37E+13	8
14	20/11/1985	17:07:22.24	1.7	127	1.10E+13	2.35
18	27/12/1985	18:00:10.63	2	163	2.51E+13	2.55
20	27/12/1985	20:07:31.85	1.2	90	2.75E+12	1.65
21	27/12/1985	20:07:49.31	1.4	152	4.79E+12	0.59
22	28/12/1985	14:52:24.25	1.9	123	1.91E+13	4.48
23	29/12/1985	19:56:02.99	1	115	1.58E+12	0.46
24	04/01/1986	02:37:06.54	1.6	107	8.32E+12	2.96
28	23/02/1986	15:33:29.42	1.5	110	6.31E+12	2.07
30	23/02/1986	15:42:31.76	1.2	202	2.75E+12	0.15
31	24/02/1986	10:09:56.51	1.5	123	6.31E+12	1.5
32	08/03/1986	03:11:28.64	1.3	125	3.63E+12	0.82
33	08/03/1986	17:39:09.65	1	103	1.58E+12	0.63
35	12/03/1986	03:34:13.93	2.2	95	4.37E+13	22.54
36	12/03/1986	03:36:04.43	2.2	157	4.37E+13	4.96
38	12/03/1986	03:54:00.19	1.9	155	1.91E+13	2.23
39	12/03/1986	05:00:06.66	1	108	1.58E+12	0.54
41	12/03/1986	05:53:25.81	2.1	147	3.31E+13	4.61
42	12/03/1986	06:58:59.54	1.7	178	1.10E+13	0.85
44	12/03/1986	15:21:38.95	1.4	107	4.79E+12	1.71
45	12/03/1986	18:55:09.54	1.5	124	6.31E+12	1.43
49	17/06/1986	18:46:00.44	2	159	2.51E+13	2.74
50	17/07/1986	07:30:31.86	1.2	73	2.75E+12	3.15
55	24/08/1986	02:38:37.50	1.1	131	2.09E+12	0.41
56	24/08/1986	02:52:31.69	1.1	102	2.09E+12	0.86
57	24/08/1986	20:13:25.54	1.5	120	6.31E+12	1.59
58	26/08/1986	06:54:18.47	1.6	119	8.32E+12	2.18
59	26/08/1986	14:15:29.71	1.1	102	2.09E+12	0.87
60	23/09/1986	20:20:35.27	1.1	145	2.09E+12	0.3

Table V. (*continued*).

N°	Date	Orig. Time	M_L	L (m)	M_0 (N m)	Δσ (bars)
61	19/10/1986	04:09:52.22	1.3	104	3.63E+12	1.43
64	27/11/1986	19:26:51.38	1.1	101	2.09E+12	0.88
67	16/12/1986	02:13:16.01	1.7	117	1.10E+13	2.99
72	03/05/1987	04:07:40.12	1.7	145	1.10E+13	1.58
73	12/05/1987	11:34:11.23	1.2	102	2.75E+12	1.12
74	12/05/1987	11:36:06.70	1.4	117	4.79E+12	1.31
77	12/05/1987	12:14:59.85	1.7	114	1.10E+13	3.28
78	12/05/1987	12:17:39.33	1.5	178	6.31E+12	0.49
80	12/05/1987	12:28:38.11	2	136	2.51E+13	4.39
84	14/06/1987	18:24:08.19	2	138	2.51E+13	4.15
89	18/12/1987	21:17:29.50	1.3	72	3.63E+12	4.3
90	24/01/1988	01:50:50.12	3	217	3.98E+14	17.13
91	24/01/1988	18:45:36.87	1.7	157	1.10E+13	1.23
96	02/05/1988	02:41:02.81	1.6	111	8.32E+12	2.63
101	21/07/1988	10:18:59.62	1.3	137	3.63E+12	0.61
105	11/01/1989	11:36:36.58	1.1	122	2.09E+12	0.5
107	07/03/1989	18:52:03.75	1	106	1.58E+12	0.58
108	09/03/1989	16:41:41.39	1.5	135	6.31E+12	1.13
109	29/05/1989	18:59:47.09	1	48	1.58E+12	6.12
111	04/06/1989	02:20:47.67	1.1	110	2.09E+12	0.68
112	04/06/1989	22:36:21.41	1.5	134	6.31E+12	1.15
113	04/06/1989	22:58:02.94	1	109	1.58E+12	0.53
114	04/06/1989	23:56:18.07	1.2	150	2.75E+12	0.36
115	04/06/1989	23:57:03.76	1.6	113	8.32E+12	2.49
116	05/06/1989	04:09:21.01	1.6	87	8.32E+12	5.53
117	06/06/1989	00:06:36.62	1.1	133	2.09E+12	0.39
127	26/08/1989	09:40:08.65	1.4	89	4.79E+12	2.95
128	13/12/1989	18:35:49.30	1.9	101	1.91E+13	8.2
129	21/12/1989	09:00:32.11	1.5	117	6.31E+12	1.72
130	21/12/1989	11:20:23.95	2.2	140	4.37E+13	6.97
131	21/12/1989	12:21:35.23	1.2	106	2.75E+12	1.01
133	31/01/1990	21:38:04.83	1.8	148	1.45E+13	1.93

Table V. (*continued*).

N°	Date	Orig. Time	M_L	L (m)	M_0 (N m)	$\Delta\sigma$ (bars)
134	31/01/1990	21:38:17.50	1.6	134	8.32E+12	1.51
136	01/02/1990	00:47:27.58	1.5	92	6.31E+12	3.51
137	01/02/1990	01:31:18.08	2.1	58	3.31E+13	74.52
138	01/02/1990	03:17:57.13	1.3	86	3.63E+12	2.52
139	01/02/1990	03:25:16.57	1.2	121	2.75E+12	0.68
140	01/02/1990	03:36:09.93	1.9	139	1.91E+13	3.11
141	01/02/1990	04:43:30.58	1.3	154	3.63E+12	0.43
142	01/02/1990	04:53:20.05	1.1	174	2.09E+12	0.17
143	01/02/1990	05:04:25.49	1.6	168	8.32E+12	0.76
145	01/02/1990	06:12:50.19	1.9	73	1.91E+13	21.36
146	01/02/1990	06:54:18.82	2	197	2.51E+13	1.43
149	01/02/1990	18:44:58.38	1.9	170	1.91E+13	1.7
151	02/02/1990	05:41:31.89	1.1	26	2.09E+12	53.29
152	02/02/1990	20:12:47.40	1.2	85	2.75E+12	1.99
157	11/02/1990	21:29:07.67	2.4	213	7.59E+13	3.45
158	28/02/1990	22:09:46.68	1.3	124	3.63E+12	0.83
159	12/03/1990	19:10:16.12	1.1	111	2.09E+12	0.67
160	16/05/1990	21:33:08.97	1	49	1.58E+12	6
163	29/09/1990	20:39:35.05	2.2	208	4.37E+13	2.12
164	29/09/1990	21:39:11.39	2.5	161	1.00E+14	10.46
168	31/01/1991	06:57:55.05	2	137	2.51E+13	4.32
169	10/03/1991	10:35:10.98	1.7	132	1.10E+13	2.08
170	20/04/1991	03:26:20.14	1.5	134	6.31E+12	1.15
246	02/07/1993	16:17:51.98	1.5	20	1.58E+12	0.15

0.9 V_S. On the basis of equation (3.2), source radii have been rescaled by assuming V_r=0.6 V_S. The resulting average stress drop is 15 bars, against the 5 bars average value obtained assuming V_r=0.9 V_S. Therefore, stress drop values of most of the analysed events remain low, even changing the velocity rupture.

Possible differences among the scaling relationships of source parameters for earthquakes of different faulting mechanisms were also investigated.

The plot of source radius vs. seismic moment for dip-slip and strike-slip fault mechanisms is shown in fig. 7c.

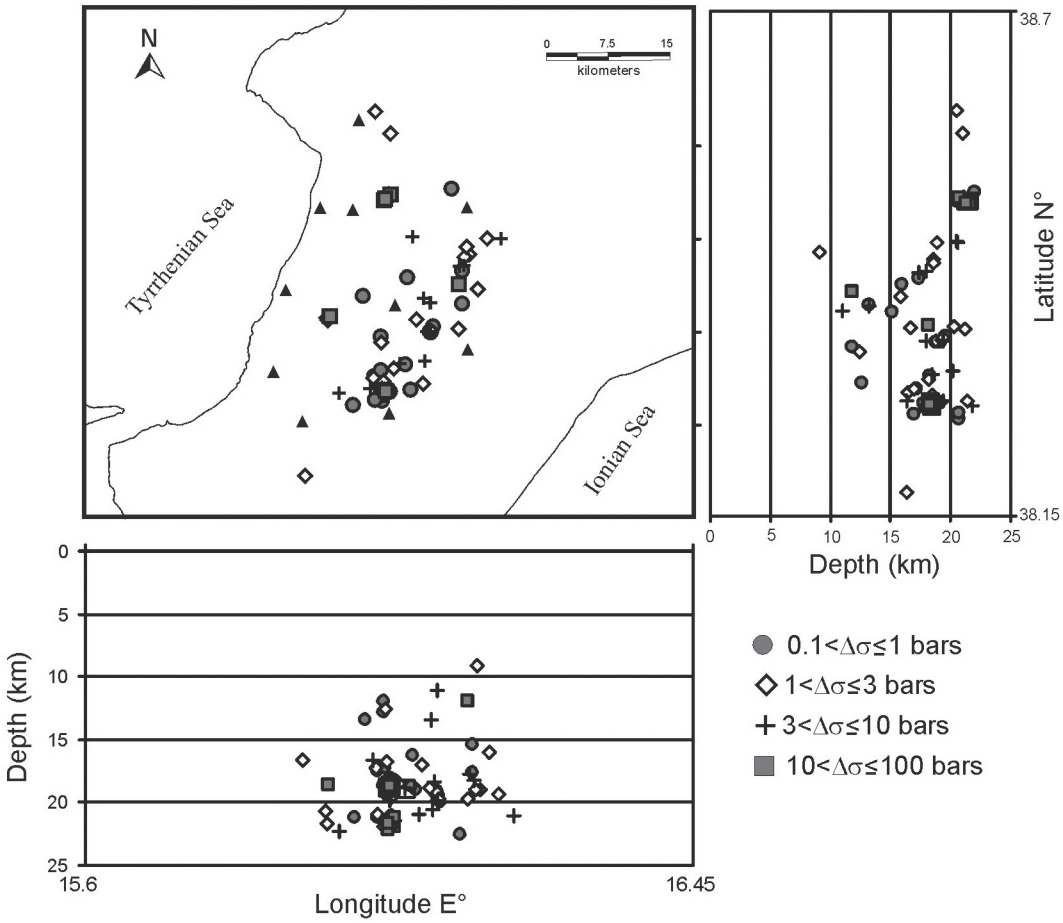

Fig. 8. Map and cross sections showing the spatial distribution of stress drop for the analysed events.

4. Discussion and conclusions

Data from a 9-year time span recorded by a temporary network deployed in southern Calabria from 1985 to 1994 were analyzed for earthquake focal mechanisms, stress tensor inversion, P-wave seismic attenuation and earthquake source parameters estimation. Although the seismic activity analyzed in this study may not be representative of the seismic behaviour of the whole area, we believe that the findings of this study may have some noteworthy implications for the prediction of the style of faulting of the region and for the comprehension of earthquake source physics.

Epicentral distribution of selected dataset (figs. 1 and 3) displays a clustering of events along a NE-SW trend, which corresponds to a segment of the well-documented Cittanova fault. The NW-SE and SW-NE cross sections (fig. 3) indicate that the depth of seismicity generally extends to about 25 km, with depth mainly concentrated from 10 to 25 km. Looking at the focal mechanisms of the events two main classes of solutions may be recognized: normal and strike-slip solutions. Normal slip solutions slightly prevail over the other. In gen-

eral, the choice of the fault plane is problematic, except when there is a clear morphological evidence of the fault at the surface and/or the epicentral distribution is well constrained and shows a clear elongation (Patanè and Privitera, 2001). In our case, FPSs show prevalent rupture orientations occurring along ca. NE-SW directions (fig. 2), in agreement with the overall distribution of foci (fig. 3) and structural setting (fig. 1). Moreover, the spatial distribution of the deformation axes (fig. 2) shows a strong dispersion for the P-axes with a maximum in the N40°-60°E class. Conversely, the prevalence of the T-axes in the N300°-320°E is well evidenced. Both strike-slip and dip-slip solutions show deformation axes with dips generally less than 60°. No systematic variations of solutions with depth are observed.

The inversion of the whole dataset of focal mechanisms for stress tensor parameters gives an average misfit of 6.2° that, on the basis of the error analysis, is near the value between acceptable and suspect results (6°) (Cocina *et al*., 1997). After dividing the entire dataset in two sub-volumes as a function of space, we found that the quality of the inversion was improved. In particular, the minimum compressive stress σ_3, estimated by stress inversion of the events located along the CF is horizontal and oriented N145E, while σ_1 is close to the vertical (76° plunge). The inversion of the 37 remaining events, located westward and northwestward of CF, again gives a horizontal σ_3, oriented approximately WNW-ESE, although with larger confidence regions.

The hypocentral distribution, the prevalence of focal mechanisms with fault planes striking about NE-SW, as well as the P- and T-axes distribution suggest that earthquakes occur along structures oriented ca. NE-SW, where surface evidence of this tectonic element is well recognized, and that the local stress field acting in this sector of the Southern Calabria is prevalently transtensional and strongly controlled by local fault heterogeneities. Interestingly, structural analysis, carried out by Tortorici *et al*. (1995) within the cataclastic belt developing along the CF, show N25-45°E trending minor fault planes characterized by subvertical slickensides (pitches ranging between 50° and 90°), indicating N140°E oriented extension (fig. 3d).

Analysis of focal mechanisms and seismogenic stress regimes carried out at regional scale in southern Italy (Frepoli and Amato, 2000a,b; Neri *et al*., 2003) and GPS results (Hollenstein *et al*., 2003; D'Agostino and Selvaggi, 2004) corroborate the hypothesis that the regional stress in the study area is dominated by a NW extension.

As concerns seismic attenuation, we found an average Q_P =84±8, which is lower than the Q_P values observed in other tectonic areas (*e.g*., Giampiccolo *et al*., 2003). This suggests a high attenuation in southern Calabria which could be interpreted as due to a high degree of cracking and/or to the presence of fluids in the fractures. In addition, we observe some lateral variability of Q_P among closely located stations. Figure 9 compares the Q_P values along the source-to-receiver path obtained at each station with the information on P-waves 3D velocity tomography performed in the region between 2 and 12 km of depth (Raffaele *et al*., 2006). In general, we observe a good agreement between both studies. In particular, high attenuation values (*e.g*. at stations DLV and CGT) well match with low V_P volumes, whereas low attenuation (*e.g*. at station STC) is found in correspondence of high V_P regions. Raffaele *et al*. (2006) interpreted the observed P-wave velocity anomalies in terms of geologic characteristics of the region. Following their interpretation, the observed P-wave anomalies may be attributed to the different percentages of major minerals in the rocks and to the respective single crystal velocities (Kern and Schenk, 1985). In fact, high contents of garnet, sillimanite, pyroxene and anphibole would produce high velocities and then low attenuation. On the other hand, material with low seismic velocities and high attenuation corresponds to rocks with low metamorphic grade. Moreover, the low Q_P observed in the proximity of the CF (*e.g*. at station DLV), corresponding to negative V_P anomaly, is in agreement with the interpretation of a zone of intense fracturing of fault gouge (Raffaele *et al*., 2006). This favours the hypothesis that the CF is a fault zone which gives rise to seismic activity.

Finally, source parameters of the earthquakes analysed are of the same order as those

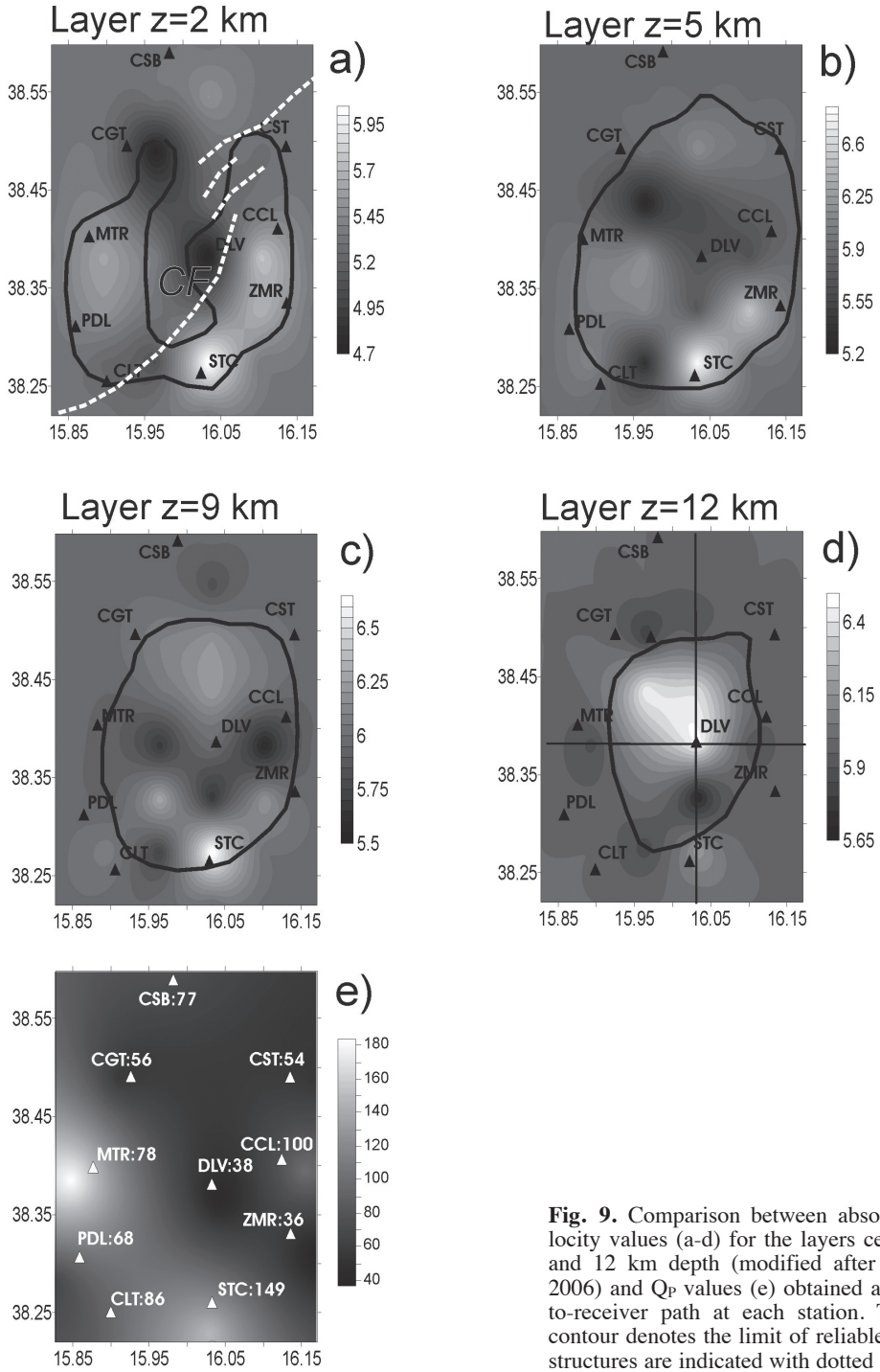

Fig. 9. Comparison between absolute P-wave velocity values (a-d) for the layers centred on 2, 5, 9 and 12 km depth (modified after Raffaele *et al*., 2006) and Q_P values (e) obtained along the source-to-receiver path at each station. The thick black contour denotes the limit of reliable resolution. In a structures are indicated with dotted white lines.

reported in literature for other datasets of microearthquakes recorded in southern Calabria (*e.g.* Patanè *et al.*, 1997) and in other tectonic settings (*e.g.*, Abercrombie, 1995; Prejean and Ellsworth, 2001; Hough and Kanamori, 2002; de Lorenzo *et al.*, 2004).

One interesting result regards the low stress drop estimates obtained for the selected earthquakes. In fact, most of the stress drop values are below 10 bars, except a few events that have stress drop up to 100 bars (fig.7a,b; table V). Looking at the spatial distribution of stress drop (fig. 8), there is no evidence of any dependence on latitude, longitude and depth. Therefore, the general low values outline a characteristic of the whole region and are indicative of crustal heterogeneities, such as low-strength structures (*e.g.* fault segments and/or weakened zones), where great stress accumulation is hindered. Since the rupture process on fault zones is heterogeneous, our findings are consistent with repeated ruptures of weak edge regions and, at the same time, do not exclude the presence of «strong» asperities were large stresses can be released (*e.g.* Sammis and Rice, 2001).

Computed source parameters allowed us to outline some scaling relationships for small earthquakes occurring in this tectonic area. From the obtained seismic moment-radius and seismic moment-stress drop relations it seems that, in the considered range of magnitude, the seismic moment increases with increasing source dimension and stress drop (fig. 7a,b). This observation implies a breakdown in the similarity of rupture processes for small earthquakes in the Gioia Tauro basin, as also observed by several authors worldwide (*e.g.* Izutani and Kanamori, 2001; de Lorenzo *et al.*, 2004; Garcìa Garcìa *et al.*, 2004), and favours the hypothesis that source processes of small earthquakes significantly differ from those of moderate to large events. On the other hand, plots of source dimension vs. seismic moment for dip-slip and strike-slip faults (the two faulting mechanisms mainly represented in the area) show the absence of any difference in the scaling behaviour (fig. 7c). Therefore, unlike moderate to large earthquakes, our results suggest that small earthquakes scale in the same manner, independently of faulting mechanism (*e.g.* Stock and Smith, 2001).

In conclusion, based on the findings of the present study we believe that the seismic activity in the study period reproduced fairly well the general features of seismicity in this specific area, even though other important seismogenic faults may have been inactive in such a relatively short period of time. In fact, seismogenic stress found to act over a 9-year time span is coherent with the main stress field inferred from geological data. This suggests that seismicity was produced by minor fault segments activated by the main stress field working in the whole region. However, to better constrain the seismotectonics of this high seismic risk area more data are needed and a more accurate knowledge of the crustal structure through high resolution investigations (*e.g.* velocity and attenuation tomographies) is required. To this end, continuing operation and technical improvement of existing earthquake monitoring networks (*e.g.* with a dense distribution of digital three-component seismic stations in key areas) should be planned in the future in order to improve the definition of specific structures and tectonic features.

Acknowledgments

We are grateful to ISMES for providing original data. We also thank Francesca Vella for her contribution in the data analysis and Giuseppe Di Grazia for helpful discussions. F.F. and S.G. have been supported by Catania University grants (Fondi di Ateneo-2005). Dr. R. Console, Prof. I. Guerra and two anonymous referees are gratefully acknowledged for useful comments and suggestions.

REFERENCES

Abercrombie, R.E. (1995): Earthquake source scaling relationship from -1 to 5 M_L using seismograms recorded at 2.5-km depth, *J. Geophys. Res.*, **100**, 24.015-24.036.

Bakun, W.H. and A. Lindth (1977): Local magnitudes, seismic moments and coda durations for earthquakes near Oroville, California, *Bull. Seism. Soc. Am.*, **65**, 615-630.

BOATWRIGHT, J. (1980): A spectral theory for circular seismic sources; simple estimates of source dimension, dynamic stress drop and radiated seismic energy, *Bull. Seism. Soc. Am.*, **70**, 1-27.

BOSCHI, E., E. GUIDOBONI, G. FERRARI, D. MARIOTTI and G. VALENSISE (2000): Catalogue of strong italian earthquakes, *Ann. Geofis.*, **43**, 268.

COCINA, O., G. NERI, E. PRIVITERA and S. SPAMPINATO (1997): Stress tensor computations in the Mount Etna area (southern Italy) and tectonic implications, *J. Geodyn.*, **23**, 109-127.

D'AGOSTINO, N. and G. SELVAGGI (2004): Crustal motion along the Eurasia-Nubia plate boundary in the Calabrian Arc and Sicily and active extension in the Messina Straits from GPS measurements, *J. Geophys. Res.*, **109**, B11402, doi:10.1029/2004JB002998.

DE LORENZO, S., G. DI GRAZIA, E. GIAMPICCOLO, S. GRESTA, H. LANGER, G. TUSA and A. URSINO (2004): Source and Qp parameters from pulse width inversion of microearthquake data in southeastern Sicily, Italy, *J. Geophys. Res.*, **109**, B07308, doi:10.1029/2003JB002577.

DI GRAZIA, G., H. LANGER, A. URSINO, L. SCARFÌ and S. GRESTA (2001): On the estimate of earthquake magnitude at a local seismic network, *Ann. Geofis.*, **44**, 579-591.

FREPOLI, A. and A. AMATO (2000a): Fault plane solutions of crustal earthquakes in Southern Italy (1988-1995): seismotectonic implications, *Ann. Geofis.*, **43**, 437-467.

FREPOLI, A. and A. AMATO (2000b): Spatial variation in stresses in peninsular Italy and Sicily from background seismicity, *Tectonophysics*, **317**, 109-124.

GALLI, P. and V. BOSI (2002): Paleoseismology along the Cittanova fault: Implications for seismotectonics and earthquake recurrence in Calabria (southern Italy), *J. Geophys. Res.*, **92**, 1029-1048.

GALLI, P., and V. BOSI (2003): Catastrophic 1638 earthquakes in Calabria (southern Italy). New insight from paleoseismological investigation, *J. Geophys. Res.*, **108**, B1, doi:10.1029/2002JB0171.

GARCIA GARCIA J.M., M.D. ROMACHO and A. JIMÉNEZ (2004): Determination of near-surface attenuation, with $\varkappa$ parameter, to obtain the seismic moment, stress drop, source dimension and seismic energy for microearthquakes in the Granada Basin (Southern Spain), *Phys. Earth Planet. Interiors*, **141**, 9-26.

GEPHART, J.W. (1990): Stress and the direction of slip on fault planes, *Tectonics.*, **9**, 845-858.

GEPHART, J.W. and D.W. FORSYTH (1984): An improved method for determining the regional stress tensor using earthquake focal mechanism data: application to the San Fernando earthquake sequence, *J. Geophys. Res.*, **89**, 9305-9320.

GIAMPICCOLO, E., S. GRESTA and G. GANCI (2003): Attenuation of body waves in southeastern Sicily (Italy), *Phys. Earth Planet. Inter.*, **135**, 267-279.

GILLARD, D., M: WYSS and P. OKUBO (1996): Type of faulting and orientation of stress and strain as a function of space and time in Kilauea's south flank, Hawaii, *J. Geophys. Res.*, **101**, 16025-16042.

GLADWIN, M.T. and F.D. STACEY (1974): Anelastic degradation of acoustic pulses in rock, *Phys. Earth Planet. Interiors*, **8**, 332-336.

HOLLENSTEIN, C., H.G. KAHLE, A. GEIGER, S. JENNY, S. GOES and D. GIARDINI (2003): New GPS constraints on the Africa-Eurasia plate boundary zone in southern Italy, *Geophys. Res. Lett.*, **30**, doi: 10.1029/2003GL 017554.

HOUGH, S.E. and H. KANAMORI (2002): Source properties of earthquakes near the Salton Sea triggered by the 16 October 1999 M7.1 Hector Mine, California, earthquake, *Bull. Seism. Soc. Am.*, **92**, 1281-1289.

IZUTANI, Y. and H. KANAMORI (2001): Scale dependence of seismic energy-to-moment ratio for strike-slip earthquakes in Japan, *Geophys. Res. Lett.*, **28**, 4007-4010.

KEILIS-BOROK,V.I. (1959): On the estimation of the displacement in an earthquake source and of source dimension, *Ann. Geofis.*, **12**, 205-214.

KERN, H. and V. SCHENK (1985): Elastic wave velocities in rocks from a lower crustal section in Southern Calabria (Italy), *Phys. Earth Planet. Interiors*, **40**, 147-160.

KJARTANSSON, E. (1979): Constant Q-wave propagation and attenuation, *J. Geophys. Res.*, **84**, 4737-4748.

LAHR, J.C. (1989): HYPOELLIPSE: A computer program for determining local earthquake hypocentral parameters, magnitude, and first motion pattern, USGS Open File Rept., **23/89**, pp. 112.

MADARIAGA, R. (1976): Dynamics of an expanding circular fault, *Bull. Seism. Soc. Am.*, **66**, 639-666.

MICHAEL, A.J. (1987): Use of focal mechanisms to determine stress: a control study, *J. Geophys. Res.*, **92**, 357-368.

MOIA, F. (1987): Analisi sulla fenomenologia sismica del maggio 1985 avvenuta nello stretto di Messina ed osservata dalla rete sismica di Gioia Tauro, (VI Conf. G.N.G.T.S., Roma), 185-194 (in italian).

MONACO C. and L. TORTORICI (2000): Active faulting in the Calabrian Arc and eastern Sicily, *J. Geodynamics*, **29**, 407-424.

MULARGIA, F. and R.J. GELLER (eds), (2003): Earthquake Science and Seismic Risk Reduction (Nato Science Series IV: Earth and Environmental Science-vol. 32), (Kluwer Academic Publisher).

NERI, G., G. BARBERI, B. ORECCHIO and A. MOSTACCIO (2003): Seismic strain and seismogenic stress regime in the crust of the southern Thyrrenian region, *Earth Planet. Sci. Lett.*, **213**, 97-112.

PARKER, R.L. and M.K. MCNUTT (1980): Statistics for the one norm misfit measure, *J. Geophys. Res.*, **85**, 4429-4430.

PATANÈ, D., F. FERRUCCI, E. GIAMPICCOLO and L. SCARAMUZZINO (1997): Source scaling of microearthquakes at Mt. Etna volcano and in the Calabrian Arc (southern Italy), *Geophys. Res. Lett.*, **24**, 1879-1882.

PATANÈ, D. and E. PRIVITERA (2001): Seismicity related to 1989 and 1991-93 Mt. Etna (Italy) eruptions: kinematic constraints by fault solution analysis, *J. Volcanol. Geotherm. Res.*, **109**, 77-98.

PREJEAN S.G. and W. ELLSWORTH (2001): Observations of earthquakes source parameters at 2 km depth in the Long Valley Caldera, eastern California, *Bull. Seism. Soc. Am.*, **91**, 165-177.

RAFFAELE, R., H. LANGER, S. GRESTA and F. MOIA (2006): Tomographic inversion of local earthquake data from the Gioia Tauro basin (southwestern Calabria, Italy), *Geophys. J. Int.*, **165**, 167-179.

REASENBERG, P.A. and D. OPPENHEIMER (1985): Fortran computer programs for calculating and displaying earthquake fault-plane solutions, USGS Open File Rept., **379/85**, pp. 109.

RICHTER, C. (1935): An instrumental earthquake magnitude scale, *Bull. Seism. Soc. Am.*, **25**, 1-32.

TORTORICI, L., C. MONACO, C. TANSI and O. COCINA (1995): Recent and active tectonics in the Calabrian Arc (Southern Italy), *Tectonophysics*, **243**, 37-55.

SAMMIS, C.G. and J.R. RICE (2001): Repeating Earthquakes as Low-Stress-Drop Events at a Border between Locked and Creeping Fault Patches, *Bull. Seism. Soc. Am.*, **91**, 532-537.

STOCK, C. and G.C. EUAN SMITH (2001): Evidence for different scaling of earthquake source parameters for large earthquakes depending on focal mechanism, *Geophys J. Int.*, **143**, 157-162.

VALENSISE, G. and G. D'ADDEZIO (1994): Il contributo della geologia di superfice all'identificazione delle strutture sismogenetiche della Piana di Gioia Tauro, Istituto Nazionale di Geofisica, *Internal Report*, **559**, 21 (in italian).

WALLACE, R.E. (1977): Profiles and ages of young fault scarps, north-central Nevada, *Geol. Soc. Am. Bull.*, **88**, 1267-1281.

WU, H. and J.M. LEES (1996): Attenuation of Coso geothermal area, California, from wave pulse width, *Bull. Seism. Soc. Am.*, **5**, 1574-1590.

WYSS, M., B. LIANG, W.R. TANIGAWA and W. XIAOPING (1992): Comparison of orientations of stress and strain tensor based on fault plane solutions in Kaoiki, Hawaii, *J. Geophys. Res.*, **97**, 4769-4790.

ZOLLO, A. and S. DE LORENZO (2001): Source parameters and three-dimensional attenuation structure from the inversion of microearthquake pulse width data: Method and synthetic tests, *J. Geophys. Res.*, **106**, 16287-16306.

(received March 27, 2008;
accepted September 18, 2008)